



Mechanical Design of a Formula Student Electric Motor

Bruno António dos Santos Fernandes

Thesis to obtain the Master of Science Degree in

Mechanical Engineering

Supervisor: Prof. Luís Alberto Gonçalves de Sousa

Examination Committee

Chairperson: Prof. João Orlando Marques Gameiro Folgado

Supervisor: Prof. Luís Alberto Gonçalves de Sousa

Member of the Committee: Prof. Agostinho Rui Alves da Fonseca

November 2019

Acknowledgments

To everyone I came across with in my years as a member of *FST Lisboa*, for the headaches, challenges and friendships created.

To my thesis supervisor Professor Luís Alberto Goncalves de Sousa, for allowing me to do this work and for all his help and serious talks across the years.

To my friends looking out for me.

To my family for their patience and support during the hard times.

Resumo

O desenvolvimento próprio dos seus próprios motores é um novo desafio para as equipas de Formula Student, não há muitas soluções disponíveis no mercado para este tipo de competição. A equipa Formula Student Técnico (FST) Lisboa aceitou este desafio de desenvolver motores próprios e já conta com um protótipo anteriormente construído. O trabalho desenvolvido nesta tese começa com a produção, montagem e teste de um protótipo de segunda geração projetado ainda no âmbito da área técnica de Propulsão. Durante a produção e montagem, foram encontrados problemas que vieram a limitar o desempenho do motor. Paralelamente à produção, uma bancada de testes foi projetada e construída. Com o motor completo e a bancada de testes operacional, uma bateria de teste foi realizada para determinar as características do motor.

Com todo o conhecimento adquirido de cada passo anterior, foram modelados sete novos conceitos - quatro referentes a preocupações eletromagnéticas e três referentes ao arrefecimento do motor. Com modelos de elementos finitos (eletromagnéticos e térmicos) para analisar cada conceito, os melhores foram escolhidos. Esse conceito foi desenvolvido e um motor completo modelado, as principais análises estruturais foram realizadas com software de elementos finitos para todos os componentes críticos. Além disso, houve grande ênfase na acomodação elétrica e mecânica de todos os componentes. É ainda apresentado um plano/conjunto de tarefas envolvidas no projeto e produção do motor.

Palavras-chave: Motor elétrico, Projeto Mecânico, Formula Student; Manufatura

Abstract

Self-developing their own motors is a new challenge concerning for Formula Student teams, there're not many solutions available on the market for this type of competition. Formula Student Técnico (FST) Lisboa took this challenge and is working on their own motors with one prototype previously built. This work begins with the manufacturing, assembling and testing of a second-generation prototype designed by the Powertrain technical area. While manufacturing and assembling, problems that would limit the motor performance were found. Parallel to the manufacturing, a test bench was projected and built. With the motor assembled and the test bench operational, a battery of test was performed to determine the characteristics of the motor.

With all the knowledge acquired with every step before, seven new concepts were modelled – four regarding electromagnetic concerns and three regarding the cooling of the motor. With finite elements models (electromagnetic and thermal) to analyze each concept, the best ones were chosen. This concept was developed, and a complete motor modelled, and major structural analysis was performed with finite element software to every critical component. Besides, there was a major emphasis on electrical and mechanical accommodation of every component. Also, a plan/tasks involved with the motor design and production are presented.

Keywords: Electric motor, Mechanical Design, Formula Student; Manufacturing

Contents

1	Introduction	1
1.1	Motivation	1
1.2	State of the art	2
1.3	Objectives	4
1.4	Structure	5
2	Second Generation Motor Prototype	6
2.1	Manufacturing	6
2.2	Assembly	9
2.2.1	Rotor and Magnets insertion	9
2.2.2	Stator insertion	10
2.2.3	Winding.....	11
2.2.4	Overall assembly	12
2.3	Bench Testing.....	13
2.3.1	General Inspections.....	14
2.3.2	Earth continuity and Grounding Test.....	14
2.3.3	Winding continuity and Insulation test	15
2.3.4	No-load test	15
2.3.5	Short-circuit test.....	16
2.3.6	Loaded test.....	17
2.3.7	Saturation Problem Testing.....	19
2.3.8	Cooling	21
2.4	Testing conclusions	22
3	Design Process	23
3.1	Introduction	23
3.2	Specifications and requirements	25
3.3	Concepts	27
3.3.1	Stator, Rotor and shaft	27
3.3.1.1	Concept 1	27
3.3.1.2	Concept 2	28
3.3.1.3	Concept 3	28

3.3.1.4	Concept 4	29
3.3.2	Motor and cooling housing	29
3.3.2.1	Concept 5	29
3.3.2.2	Concept 6	30
3.3.2.3	Concept 7	30
4	Electromagnetic analysis	31
4.1	Finite Element Analysis	31
4.1.1	Geometry	31
4.1.2	Material properties	31
4.1.3	Boundary Conditions	31
4.1.4	Mesh	31
4.1.5	Simulation	31
4.2	Results	32
5	Thermal analysis	35
5.1	Finite Element Analysis	35
5.1.1	Geometry	35
5.1.2	Material properties	35
5.1.3	Boundary Conditions	35
5.1.4	Mesh	35
5.1.5	Simulation	36
5.2	Results	37
6	Mechanical Design	39
6.1	Shaft	39
6.2	Rotor	46
6.3	Stator	51
6.4	Housing	53
6.5	Lids and supports	54
6.6	Bearings and Retainers	55
6.7	Engineering fits	57
6.8	Design, manufacturing, assembling and testing	59
7	Conclusions	62

7.1	Summary	62
7.2	Future work.....	63
8	References.....	64
9	Appendix	66
	A. Vacodur 49 Datasheet.....	66
	B. AMK specs datasheet.....	67
	C. Motor manufacturing pictures	68
	D. Bench and test pictures	73
	E. Second Generation Technical Drawings	76

List of tables

Table 2.1 - Second generation expected characteristics	6
Table 2.2 - Raw data from no-load test.....	15
Table 2.3 - Short-circuit test raw data	17
Table 2.4 – Loaded test raw data.....	18
Table 2.5 - Xd and Ld calculations	19
Table 3.1 - AMK DD5-14-10-POW - 18600-B5 specs [5]	25
Table 3.2 - Geometrical and temperature requirements	27
Table 4.1 - Estimated maximum torque results	34
Table 5.1 - Domains and Material for thermal simulation	35
Table 5.2 - Thermal analysis results	38
Table 6.1 - Shaft material properties [15][17][18][19].....	39
Table 6.2 - Stress analysis results - shaft	45
Table 6.4 - Key dimensions.....	46
Table 6.3 - Stress analysis results – rotor	48
Table 6.5 - Retainer operating conditions	57
Table 6.6 - Steps and tasks to design and build a motor.....	61

List of Figures

Figure 1.1 - Electric motor used in FST cars. From left to right: 04e - Agni Motors 95-R; 05e - Siemens 1FE1; 06e - Siemens 1FE1; 07e and 08e - AMK DD5-14-10-POW	1
Figure 1.2 - AMK motor kit (left) and Fischer motor (right)	2
Figure 1.3 - Motor type selection and Advantages diagram [2]	3
Figure 1.4 - SMPM Rotor (left) and IPM rotor (right) [4].....	4
Figure 1.5 - Spoke topology [1]	4
Figure 2.1 - Second Generation Motor: motor housing; stator and windings; rotor, shaft and magnets (from left to right)	6
Figure 2.2 - Stator and Rotor sheets with manually applied Epoxy (left) and Stator and Rotor stacked sheets with respective JIG (right)	7
Figure 2.3 - Rotor samples drying.....	7
Figure 2.4 - Machined Shaft.....	8
Figure 2.5 - Two view of the machined motor housing	8
Figure 2.6 - Shaft insertion.....	9
Figure 2.7 - Magnets insertion	10
Figure 2.8 - Stator insertion.....	10
Figure 2.9 - Homemade coils	11
Figure 2.10 - Winding homemade attempt with 3D printed plastic stator	11
Figure 2.11 - Coils inside the stator	12
Figure 2.12 - Encoder installation	12
Figure 2.13 - Complete motor	13
Figure 2.14 - Test-bench under construction	13
Figure 2.15 - Operational test-bench	14
Figure 2.16 - AMK accoupled to new prototype.....	14
Figure 2.17 - Induced voltage measure - no-load test	16
Figure 2.18 - Current measure - no-load test.....	16
Figure 2.19 - Spatial vectors and magnet flux	18
Figure 2.20 - Test-bench: capacitors, measuring devices and power supply	19
Figure 2.21 - Diagram of the circuit to trace B-H curve measurement	20
Figure 2.22 - Experimental determination of B-H curve for Vacodur 49	21
Figure 2.23 - Theoretical B-H curve for Vacodur 49 [8]	21
Figure 3.1 - Motor design processes and aspects	23
Figure 3.2 - Flow chart of motor design [7]	24
Figure 3.3 - Independent cooling housing.....	25
Figure 3.4 - AMK motor dimensions [5].....	26
Figure 3.5 - Concept 1 stator and rotor representation.....	27
Figure 3.6 - Concept 2 stator and rotor representation.....	28
Figure 3.7 - Concept 3 stator and rotor representation.....	28
Figure 3.8 - Concept 4 stator and rotor representation.....	29

Figure 3.9 - Concept 5 Chicane circuit.....	29
Figure 3.10 - Concept 6 Spiral circuit.....	30
Figure 3.11 - Concept 7 Serpent circuit and water representation	30
Figure 4.1 - Magnetic Flux density (left) and Axial torque (right) for concept 1	32
Figure 4.2 - Magnetic Flux density (left) and Axial torque (right) for concept 2	33
Figure 4.3 - Magnetic Flux density (left) and Axial torque (right) for concept 3	33
Figure 4.4 - Magnetic Flux density (left) and Axial torque (right) for concept 4	33
Figure 5.1 - Water circuit Concept 7	37
Figure 5.2 - Motor temperatures	37
Figure 6.1 - Initial iteration for Concept 4 shaft	39
Figure 6.2 - Bolts disposition example	40
Figure 6.3 - Coefficient of friction and rider wear for titanium and titanium-aluminum alloys sliding on themselves and on 440-C stainless steel [20]	41
Figure 6.4 - Von Mises stresses on shaft for torsional analysis.....	44
Figure 6.5 - Safety factor for shaft torsional analysis.....	45
Figure 6.6 - Shaft keys and keyways	46
Figure 6.7 - Von Mises stresses on rotor for torsional analysis	47
Figure 6.8 - Safety factor for rotor torsional analysis	47
Figure 6.9 - Von Mises stresses on rotor for maximum speed analysis	48
Figure 6.10 - Safety factor on rotor for maximum speed analysis	48
Figure 6.11 - Fatigue Criteria's.....	49
Figure 6.12 - Exploded view of the final shaft version	51
Figure 6.13 - Stator stacking JIG	52
Figure 6.14 - VPI process: (a) evacuating the container into deep vacuum, (b) introducing epoxy resin into the container until the stator is completely submerged, (c) releasing the vacuum of the container and applying pressure over the resin-covered stator to force resin completely into the stator, (d) draining epoxy resin out of the container, and (e) placing the stator into an oven and baking it for curing the epoxy resin (not shown). [7]	53
Figure 6.15 Water circuit	53
Figure 6.16 - Fall test housing deformation	54
Figure 6.17 - Cooling circuit lids.....	55
Figure 6.18 - Motor lid	55
Figure 6.19 - Bearing dimensions	56
Figure 6.20 - List of bearings[23]	56
Figure 6.21 - Retainer dimensions	56
Figure 6.22 - Clearance fit shaft-hole.....	57
Figure 6.23 - Final CAD model exploded view.....	59
Figure.9.1 - Stator lamination JIG	68
Figure.9.2 - Manual application of bonding Epoxy 1	68
Figure 9.3 - Manual application of bonding Epoxy 2.....	69

Figure 9.4 - Dry oven for epoxy cure.....	69
Figure 9.5 - Stator after cure	70
Figure 9.6 - Nitrogen application on shaft	70
Figure 9.7 - Epoxy application for bonding magnets.....	71
Figure 9.8 - Magnets insertion	71
Figure 9.9 - Damaged stator parts after first attempt of insertion	72
Figure 9.10 - Final parts before assembling	72
Figure 9.11 - Motor coupled to bench test	73
Figure 9.12 - Data collection	73
Figure 9.13 - Data collection 2	74
Figure 9.14 - Bench test capacitors	74
Figure 9.15 - Test bench with Invertors and cooling circuit.....	75

List of symbols

A	Heat exchanging area
A_c	Cross-section area
B_m	Magnetic flux density
B_r	Radial magnetic flux
B_θ	Tangential magnetic flux
C_m	Heat capacity
c_s	Thermal Conductivity
D	Magnetic field displacement
d_{bolt}	Bolt diameter
E	Young modulus
f	Operation frequency
F	Forces acting on the fluid
F_N	Normal force
h	Convection heat transfer coefficient
H	Magnetic field
I_i	Current of phase i
I_{ij}	Current between phase I and j
J_T	Torsion constant
K_e	Voltage constant
k_{eff}	Effective conductivity
K_t	Torque constant
L	Active length of the machine
L_q	Quadrature inductance
n	Factor of safety
N	Number of turns in the coil
n_1	Outward from object
p	Pressure
Q	Convective heat flux
r	Radius of closed surface at the motor airgap
r_{shaft}	Shaft radius
S_a	Limiting value of the amplitude stress
S_e	Endurance limit
S_f	Fatigue strength
S_u	Ultimate tensile strength S

S_y	Yield strength
T	Stress tensor
T	Temperature
T_∞	Fluid temperature
T_e	Estimated torque
T_r	Applied torque
T_s	Surface temperature
U	Strain energy
U_{ij}	Voltage between phase i and j
V	Voltage
V_e	Back EMF
X_d	Quadrature reactance
Φ_m	Magnetic flux
σ_{VM}	Von Mises stress
σ_a	Amplitude stress
σ_m	Mean stress
σ_{max}	Maximum stress
σ_{min}	Minimum stress
τ_m	Motor torque
μ	Dynamic viscosity
μ	friction coefficient
ν	Poisson ratio
ρ	Material density
ω	angular speed

List of abbreviations

AC – Alternating Current

CAD – Computer Aided Design

CNC – Computer Numerical Control

DC – Direct Current

EDM – Electric Discharge Machining

EMF – Electromotive Force

FEA – Finite Element Analysis

FSG – Formula Student Germany

FST – Formula Student Técnico

GMRES – Generalized minimal residual method

IM – Internal Magnets

IMP – Interior Permanent Magnets

MST – Maxwell Stress Tensor

PCB – Printed Circuit Board

PM – Permanent Magnets

PMM – Permanent Magnets Motor

PMSM - Permanent Magnets Synchronous Motors

PTC – Positive Temperature Coefficient

SMPM – Surface Mounted Permanent Magnets

VM – von Mises

VPI – Vacuum Pressure Impregnation

1 Introduction

1.1 Motivation

For almost 4 years of my academic career, my time was spent with the formula student team of the Instituto Superior Técnico – Formula Student Técnico (FST) Lisboa. Formula student is an engineering competition at university level, where different groups of students build formula-type cars to compete against one another at official events sponsored by the industry. During prototype development, students combine their studies with managing a small business - as such, the team is structured in several sectors (Aerodynamics, Electronics, Marketing and Management, Vehicle Dynamics, Powertrain), allowing students to develop their skills and apply technical knowledge acquired throughout their studies.

Teams and their cars are evaluated at the competitions in two categories: static and dynamic events. Regarding the first, the participants must defend their design choices against a jury usually made of engineers from the companies sponsoring the event. They must also prepare a business plan based on small business involving the car and last, the cost event that evaluates everything regarding to build and produce the car. Regarding the dynamic events, the car participates in four different events:

- Skid-pad (laps in an eight-like track with the purpose of measuring cornering speed);
- Acceleration (75m in a straight line);
- Autocross (single lap in challenging track);
- Endurance and efficiency (22 laps in a track like Autocross but here the objective is not only to be fast but also the most efficient possible regarding the energy consumption).

FST Lisboa started in 2001 and currently has nine existing prototypes. The FST04e was the first high-performance electric car developed and manufactured in Portugal, marking the transition between internal combustion cars to electric cars. This change was justified for both technological (the race for knowledge regarding electric vehicles would soon boom) and logistical reasons (it was easier to attract potential sponsors with an e-car). If we look at just the motors used since the FST04e, shown at Figure 1.1, different market solutions have been used:

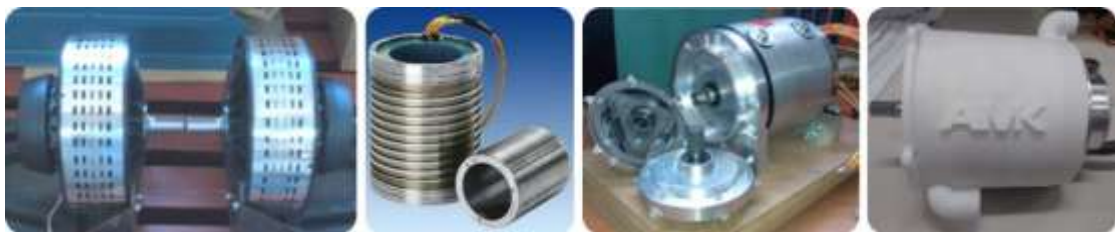


Figure 1.1 - Electric motor used in FST cars. From left to right: 04e - Agni Motors 95-R; 05e - Siemens 1FE1; 06e - Siemens 1FE1; 07e and 08e - AMK DD5-14-10-POW

The first three solutions were motors that were built and designed for other purposes and then adapted to the team's needs – which sometimes proved challenging for that reason. More recently (FST07e onward) the motors used were designed by AMK, a company which benefited from a

partnership with another formula student team. This solution was better suited for the kind of e-car we were building. However, at the same time, the challenge and motivation for designing the electric motors in-house emerged in the team. Doing so would bring several advantages: a fully customized solution (torque, weight, etc.) adapted to the car's needs could be built, costs could be reduced due to new sponsorship options, and, finally and most importantly, further knowledge and know-how could be acquired by the team. Thus, with the thesis of Eng. José Sarrico, a former team member, the project for the first self-made motor began [1]. Besides the highly appraised academic reception, the team got then a first version of the motor to test and iterate, alongside the tools used to design it. Following the first version, in which the focus was the electromagnetic design of the motor, there was a need for more attention to the mechanical design as well as its incorporation in the car. Due to initial limitations in the first iteration, the manufacturing, assembling and testing were given less focus.

The design of the second iteration was a responsibility of the division that I led in my last year in the team - Powertrain. Manpower was widely available in the beginning of the year and as such the design process was running smoothly – problems were being quickly identified and solved. However, as the year progressed, complications with the construction of the FST08e arised and all manpower had to be redirected, relegating the development of the e-motor to the background. At the end of the year, although the design was ready and some parts were in production, everything else was on stand-by. This caused me a feeling of unfinished work and because of it, despite leaving the team, I proposed to continue the challenge of finishing the work on the motor as my MSc thesis project.

1.2 State of the art

Nowadays, most competitive electric teams in Formula Student are using Alternating Current (AC) Permanent Magnets Synchronous Motors (PMSM). There are two solutions available on the market (Figure 1.2) designed specifically for the usage in Formula Student competitions.



Figure 1.2 - AMK motor kit (left) and Fischer motor (right)

The *AMK* kit is composed for a fully operational set of 4 motor and four inverters contrasting with *Fischer* which only provides the motor without shaft, bearing, encoder and inverters. A small number of teams are also designing their own but only an even smaller number has used it in real life until today.

The first prototype built, is also a PSMS and at Figure 1.3 a few advantages from each type of motor are listed:

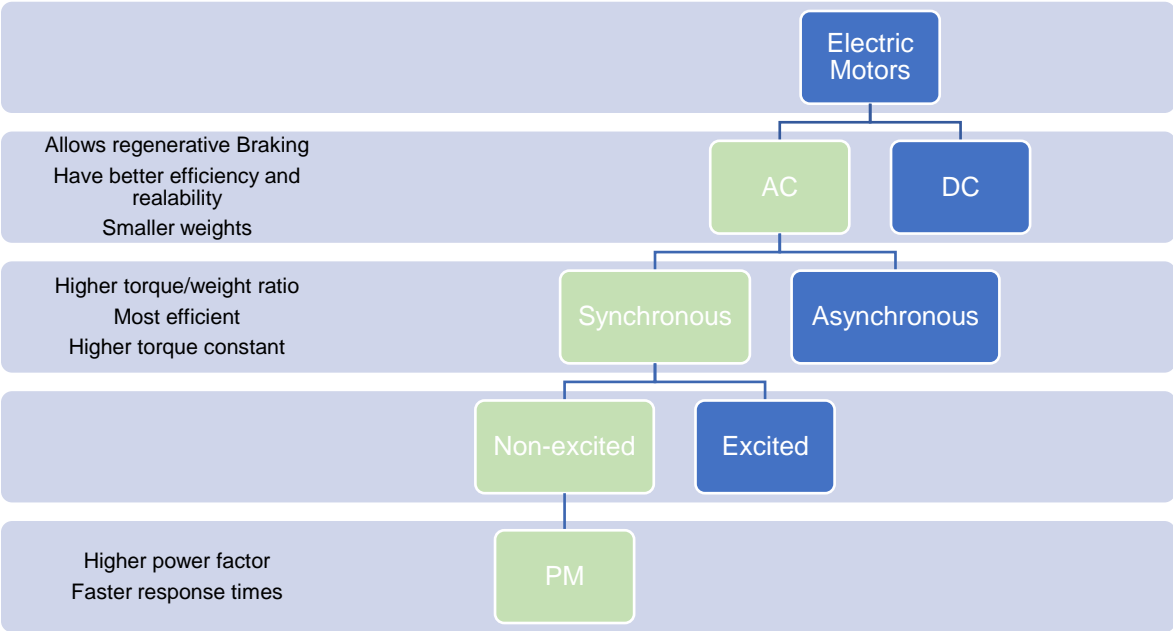


Figure 1.3 - Motor type selection and Advantages diagram [2]

Despite the advantages, this type of motors is more sensible to mechanical vibrations and high temperatures due to the possibility of crack formation or demagnetization of the permanent magnets (PM). They're also expensive than other motors due to the price of the PM.

Synchronous machines have the rotation of the shaft synchronized with the frequency of the supply current. They contain multiphase electromagnets on the stator which creates a magnetic field that rotates in time with oscillation of the supplied current, the rotor with usually permanent magnets creates another magnetic field. When current flows through the windings of the stator, it creates an electromagnet by the creation a magnetic field which rotates according to the current flowing from coil to coil over time. The magnetic provided by the PM on the rotor, is attracted to the stator rotating magnetic field, causing the rotation of the shaft and rotor. This represents one of the main forces responsible for rotation the shaft and rotor – Lorentz force. [3]

Inside PSMS we can find two different categories of rotor geometries – Surface Mounted Permanent Magnets (SMPM) or Interior Permanent Magnets (IPM) machines:

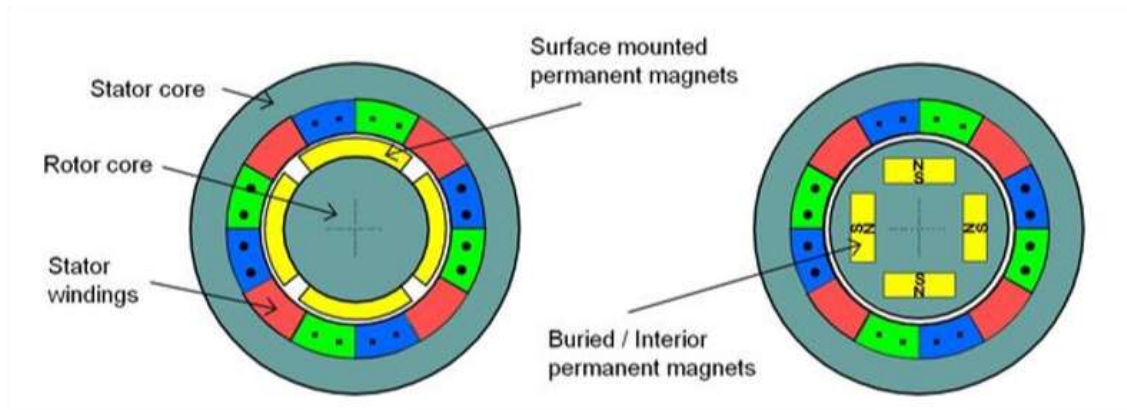


Figure 1.4 - SMPM Rotor (left) and IPM rotor (right) [4]

The first solution is more common, simpler and has lower manufacturing costs. But the magnets are more exposed to demagnetization fields and internal heat produced by Joule losses in the stator windings which affects the rotor surface and airgap. Additionally, the centripetal forces can cause detachment between the rotor and magnets.

Regarding the second, IPM machines have the possibility to concentrate the magnetic field generated inside the rotor, allowing to achieve higher airgap magnetic flux densities, which leads to increasing the motor electromagnetic torque. Since the magnets are inside the rotor, they have a better protection from mechanical vibrations and not so exposed to demagnetization fields like in SMPM.

The first prototype built and the second designed had IPM arranged in a *Spoke* topology (Figure 1.4). The same solution will be used again third prototype, the decision was made according to the advantages mentioned before. SMPM can also be obtained with materials and manufacturing processes available to the team resources. Besides it would be counterproductive to ignore the work already done in the first prototype and change everything.

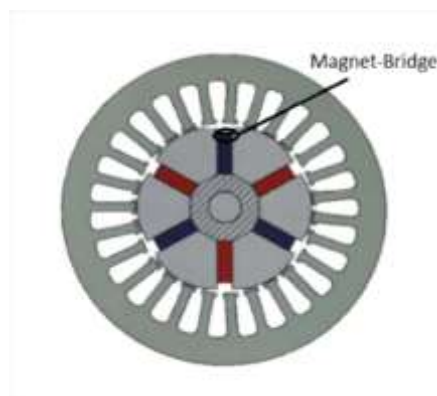


Figure 1.5 - Spoke topology [1]

1.3 Objectives

The objectives proposed with this thesis are the following:

- Manufacturing, assembly and testing of a second generation motor, designed by the FST Lisboa Powertrain team;
- Failure/success analysis of the motor second generation;
- Design of the motor third generation for integration on a previous formula student car;
- Static and fatigue studies of critical motor components;
- Propose a plan for the manufacture and assembly.

It is also my intention to provide special attention to details of accommodating both electrical and mechanical components that are often overlooked due to the immensity that is projecting the whole car from scratch.

In this project, different areas will be considered alongside mechanics: rotor and stator design - electromagnetic aspects, as well as thermodynamics in the cooling housing. All materials will be selected, all auxiliary jigs will be designed, and the manufacturing and assembly processes chosen.

In conclusion, it is my goal that with this thesis, a future team member should have all the necessary tools for designing, manufacturing and assembling a prototype of a new and better motor as well as helping with the long-term objective of having 4 self-made motors on a future FST car.

1.4 Structure

This thesis will be divided into 7 chapters including this introduction.

Chapter 2 will be about the manufacturing of the second motor prototype, its assembling and testing. In chapter 3 the design process will be mentioned, also it will be established design goals for the motor and design restrictions. With the previous, concepts to analysis and compare will also be presented.

At chapter 4, electromagnetic simulations will be addressed and at chapter 5, thermal analysis to choose the best concept.

In chapter 6, the mechanical design of the motor components will be performed based on the previous two chapter results.

To end, in the chapter 7 conclusion will be drawn.

2 Second Generation Motor Prototype

The second generation of the self-made motors was designed within the Powertrain team of FST Lisboa. It consists on a three-phased AC motor, PSMS with IPM arranged in a spoke geometry. The motor has a titanium alloy shaft, a rotor and stator made of s cobalt-iron – *Vacodur 49* with enhanced magnetic properties, neodymium PM and housing components made of aluminum alloys. The motor is water cooled. Some of the motor subassemblies can be seen at Figure 2.1, for specific dimensions, the technical drawings can be found in the annexes. One encoder for shaft position reading and temperatures sensors, mounted on the smaller body above the main body, are also part of the motor.



Figure 2.1 - Second Generation Motor: motor housing; stator and windings; rotor, shaft and magnets (from left to right)

The second generation was designed to have the characteristics summarized at Table 2.1:

Description	Value	Unit
Max Torque	18,6	Nm
Output power	29,4	kW
K_e (Voltage Constant)	27,7	(V/krpm)
K_t (Torque Constant)	0,325	Nm/A
L_d (d – axis inductance)	0,755	mH
L_q (q – axis inductance)	0,879	mH
Power factor	0,446	-

Table 2.1 - Second generation expected characteristics

2.1 Manufacturing

Both Rotor and Stator are made of a special cobalt-iron alloy, *Vacodur 49* (49 % Fe, 49 % Co, 2 % V + Nb) which comes in 0,2mm sheets with an epoxy to bod and stack until the final shape intended. The metal sheets were laser cut: this process allowed better precision given the complex geometry.

To obtain the final form of Rotor and Stator, a jig was designed and manufactured to assemble all 800 individual cut pieces (Figure 2.2) and to allow the cure of *Vacodur* epoxy (200°C during one hour in a dry environment). This first attempt to bond, brought the first big problem: the metal sheets provided to the team didn't have the epoxy. An alternative solution was needed and after consulting a few sellers of this type of alloy, the epoxy was acquired to manually be applied to every sheet.



Figure 2.2 - Stator and Rotor sheets with manually applied Epoxy (left) and Stator and Rotor stacked sheets with respective JIG (right)

The epoxy layer was supposed to be two microns thick, but manually this was impossible, just handling the sheets could damage them. The epoxy application was tested on a few samples to find the process which allowed the thinnest layer, between brushing, rolling and spraying, the last was the better one because it didn't damage the sheets like rolling and allowed thinner layers than brushing. After applying the epoxy, a small amount of heat needed to be applied to uniformize the layer. At Figure 2.3, one of the attempts to dry and uniformize can be seen.



Figure 2.3 - Rotor samples drying

The result of this problem was a reduction on the number of sheets that compose the stator and rotor. At this moment it was also predictable that the motor would underperform directly to the reduction of sheets – around 30% less from what was initially pretended.

The shaft (Figure 2.4) was designed to be manufactured in a Titanium alloy (Ti90/Ai6/V4), which proves to be harder to machine under more traditional processes when compared to steel or aluminum. Associated with complex geometry, the shaft was produced in two phases: EDM for the section where the rotor was supposed to be inserted and CNC milling for the rest.



Figure 2.4 - Machined Shaft

The second generation project represented the first attempt to join the motor and cooling housing in a single piece. Using additive manufacturing, this could be easily obtained, but the lack of resources regarding this process made it impossible. Nonetheless, having the both housings together was still possibility to be tested, it just need more creativity to design a solution to be manufactured with processes available to the team. One main component with through all vertical channels and 11 smaller lids to close the circuit after assembled in the main component were designed (see technical drawings).



Figure 2.5 - Two view of the machined motor housing

The smaller parts and lids, using an AL 6061-T6, were all milled while the main part needed EDM to open the channels of water circuit. The lids were used to cover the opening and to form a serpent like path to the water. In Figure 2.5 we can see were the channel were open with EDM looking at the black spots on the right part of the image – they are silicon used to completely seal the place where the lids were inserted.

Other parts necessary for the completion of the prototype were bought bearings, bolts, copper for winding, fittings, plugs, encoder, retainers and cables.

2.2 Assembly

2.2.1 Rotor and Magnets insertion

Due to the high velocities expected for the rotor, a forced fit was recommended (H7/u6) [10] but, with all the problems occurred during the stacking, the rotor didn't expand as expected with heating. To test if it could contract enough to ease its assembly, the shaft was submerged in nitrogen, but given its material, the result was not helpful. The solution available was to heat up the rotor and with the help of a manual press, force the shaft all the way through (Figure 2.6). It worked but it also caused a small deformation that was only identified when mounting the bearings – it was harder to insert the bearing on one side despite having the same clearance.



Figure 2.6 - Shaft insertion

The magnets had a sliding fit, but again, due to the rotor stacking problems, there was an excess of epoxy in the magnet's slots. Instead of sliding through the slot, they needed to be forced (Figure 2.7), risking breaking or damaging them – which possibly occurred, while inserting one of the eight magnets, a cracking noise was heard. The attractions between the magnets was enough to keep them in their place, but to better security, they were glued to the rotor.



Figure 2.7 - Magnets insertion

2.2.2 Stator insertion

The stator, since it is a fixed part, didn't require a fit so extreme as the rotor, the literature recommends a press fit (H7/p6) [10]. To do it, the stator was immersed in liquid nitrogen and with the help of a guiding jig, inserted into the housing. The process started ok but once 1/3 of the stator was in, it cracked and got separated in four pieces, with the biggest one inside the housing. Removing it damaged the inside a bit and repairing the stator was possible, but it lost 5% of its original height. This showed that the epoxy used in the stacking could not be operated in cold temperatures.

Since the motor housing was made of an aluminum alloy, after the stator repaired, a second try was made by heating up the housing in an oven (max. temperature – 250°C) for one hour. Again, using the guiding jig, the stator was placed and slide almost 2/3 without any help, the rest was manually pressed successfully (Figure 2.8).



Figure 2.8 - Stator insertion

2.2.3 Winding

The winding process is usually made using auxiliary machinery but, every company specialized in doing it only works with motors on totally different scales. This led to homemade attempt of preparing the windings using AWG 5 copper wire, but without the proper tools and experience the result was coils with a way less of wire than what was need (Figure 2.9). This attempt also had the objective of proving that doing this on a scale so small compared to the industry was possible (Figure 2.10).

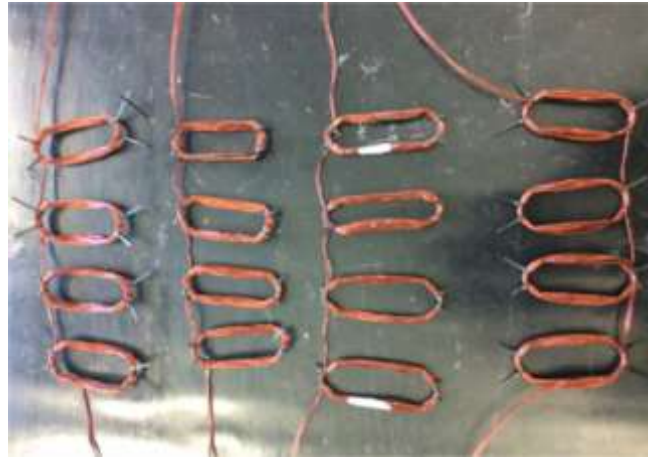


Figure 2.9 - Homemade coils



Figure 2.10 - Winding homemade attempt with 3D printed plastic stator

Eventually, a company interested with this project, offered to help. They successfully prepared the coil with the right tools (Figure 2.11). After performing the winding, the coils are submitted to Vacuum Pressure Impregnation (VPI) process. This consists on a process that uses a resin or varnish to seal porous materials using vacuum and pressure [11]. On this case, VPI removes the air between the coil's wires. This is an important step because having air between the wires can cause heating problems, having the varnish is helpful to cool down the coils easier.

But, this process is performed in tanks way too big to be economically viable to perform in a motor so small, so VPI was not done.



Figure 2.11 - Coils inside the stator

2.2.4 Overall assembly

After having all sub-assembly done, all that was missing was putting everything together. The bearings were inserted in the shaft following their manufacture instructions and with it the sub-assembly rotor and shaft was ready to be inserted inside the rotor. This was expected to be a problem due to the magnetic forces created by the magnets but turned out quite easy. The lids were screwed in place and finally the motor was ready to start test-benching. At this stage the rotor hadn't been balanced and due to the problems later presented, this would not be done.

The encoder (Figure 2.12) and its cover were mounted just to check for any problem, since it wouldn't be need for the first test, it was removed for safety. The motor was now prepared to be tested (Figure 2.13).



Figure 2.12 - Encoder installation



Figure 2.13 - Complete motor

2.3 Bench Testing

Theoretical models have errors associated, simplifications made, the way the calculations are processed or even impossibility of considering real-life problems, like manufacturing defects. Even so, physical tests are performed to validate the theoretical models and improving them.

To test the motor, a test-bench was needed (Figure 2.14). So, with the help of Powertrain area, one was built. This test-bench was designed to test one motor directly accoupled to another motor, but also had room for further improvements. It's prepared to in the future have a torque sensor or test other assembly of the car like the transmission or brake disks.



Figure 2.14 - Test-bench under construction

The test-bench was composed with a structure to set up the motor and protect the user (Figure 2.16). It incorporates part of the car cooling circuit with a pump, tubing and a radiator with a fan installed (Figure 2.15). Has a low voltage supply to power data acquisition circuit boards (PCB) and motor controllers board and has a high voltage supply to power the motors. To covert DC to AC, the car inverters are also part of the test-bench.



Figure 2.15 - Operational test-bench

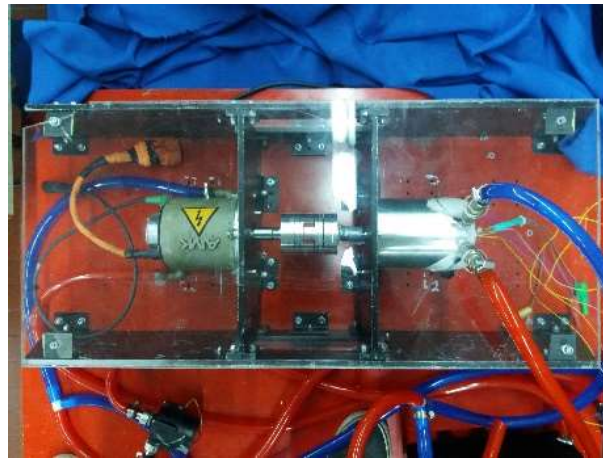


Figure 2.16 - AMK accoupled to new prototype

2.3.1 General Inspections

The first tests to be done consisted in a visual inspection and manually rotation of the motor. While visually everything seemed ok, two problems were found: there was something loose in Z-axis; by rotating the shaft a noise could be heard. Upon further investigation, the second problem was originated by a damaged bearing. This lead to disassemble the motor and look for the what caused, since it was suspected already that the shaft could have damage due to the forced insertion, the shaft and rotor were mounted on a lathe and using a dial gauge a small deformation was found. Regarding the looseness, every part dimension was checked and compared to *CAD* models, but nothing wrong was found, despite this, the problem was solved adjusting the bearing position on the shaft.

2.3.2 Earth continuity and Grounding Test

To safely operate the motors while testing it's imperative to have proper earthing, preventing electric shocks by allowing the passage of current under fault conditions. To check this, using an ohmmeter, the resistance between the motor plugs and the test-bench ground was measured – $0,1\Omega$ which is under accepted values of $0,5\Omega$ for safely operating.

2.3.3 Winding continuity and Insulation test

This test only consists on checking continuity between the three phases, if any fails it could indicate All phases combination were checked using a multimeter, and the resistance varied from 0,122Ω to 0,126Ω, which it's not relevant.

It was also check continuity between phases and the motor body, both parts were isolated – every value was up to 10MΩ.

2.3.4 No-load test

After the basic and safety tests, it was time to start charactering the prototype and to do it, a no load test was performed, using the *AMK* as motor and the prototype as generator. Using the inverters interface and the same software used in the car to control torque and speed, different steps of speed were asked to *AMK* motor while at the prototype, which was rotating at the same speed, the voltage and current values of each phase were being measured. Knowing that:

$$\omega = \frac{V_e}{K_e} \quad (2.1)$$

In which ω is the angular speed, V_e the Electromotive Force (EMF) and K_e the voltage constant [5], it can be determined experimentally:

Speed (rpm)	Uab (V)	Ubc (V)	Uca (V)	Iab (A)	Ibc (A)	Ica (A)
200	2,05	2,12	2,09	4,7	4,9	4,3
500	4,08	4,11	4,13	11,00	11,40	10,80
750	6,15	6,15	6,17	15,2	15,7	15
1000	8,21	8,21	8,23	18,3	18,8	18,1
1250	10,25	10,26	10,3	20,5	21	20,2
1500	12,31	12,31	12,35	21,8	22,3	21,4
1750	14,37	14,36	14,4	22,7	23,1	22,9
2000	16,42	16,42	16,47	-	-	-
2250	18,48	18,46	18,53	-	-	-
3000	24,65	24,61	24,71	-	-	-
3500	28,75	28,72	28,82	-	-	-
4000	32,86	32,82	32,93	-	-	-
4500	37,09	37	36,9	-	-	-
5000	41	41	40,8	-	-	-

Table 2.2 - Raw data from no-load test

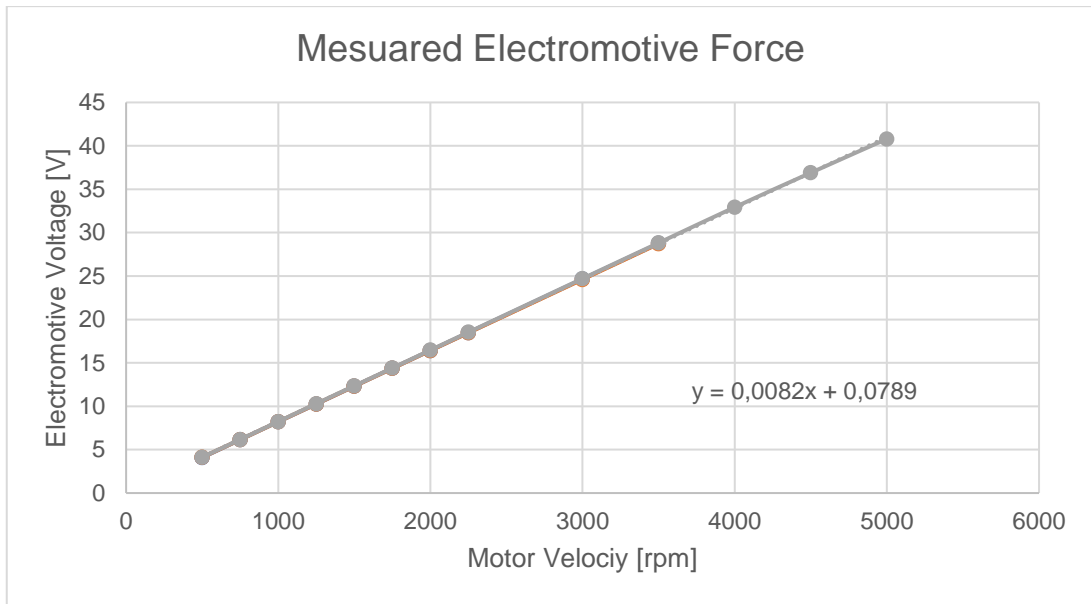


Figure 2.17 - Induced voltage measure - no-load test

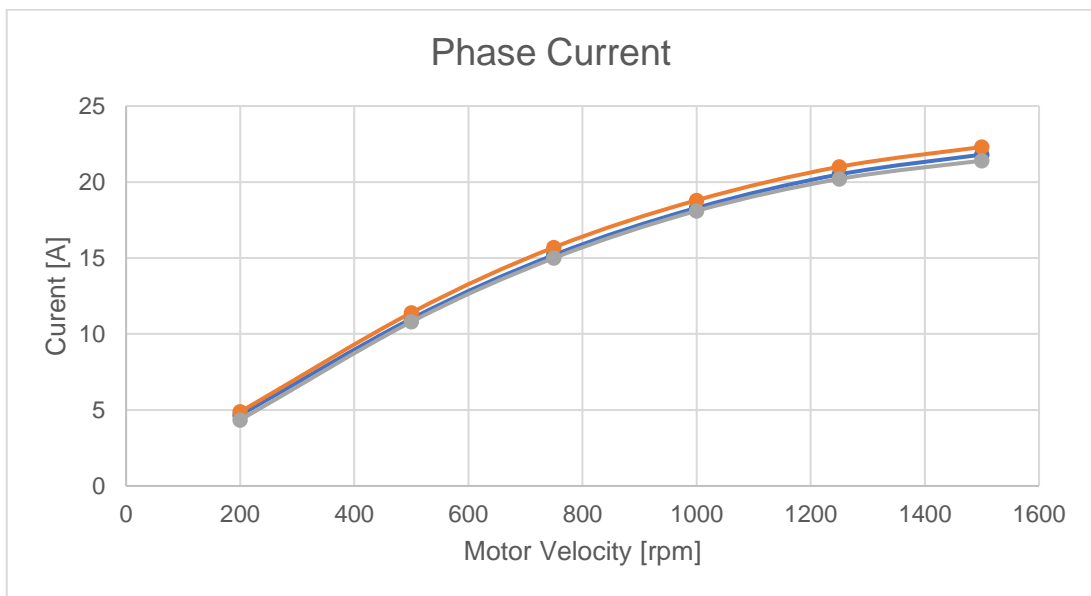


Figure 2.18 - Current measure - no-load test

Analyzing Figure 2.17, a voltage constant was extracted – $K_e = 8,2 \frac{V}{krpm}$. Also, based on Figure 2.17, the motor saturated above 1500 rpm which indicated a problem that was limiting the prototype performance.

2.3.5 Short-circuit test

The test conditions are the same as the previous test, but now with the phases connected. Since both motors are directly connect, they will have the same exact speed. The short-circuited prototype will create a resistance force for the *AMK* motor and for both motors to rotate at the same speed, the torque

used by *AMK* to move will be equal to the torque produced by the prototype. These conditions allow to estimate the Torque Constant, K_t :

$$K_t = \frac{\tau_m}{I_a} \quad (2.2)$$

$$\frac{K_t \text{ AMK}}{K_t \text{ Prototype}} = \frac{\frac{\tau \text{ AMK}}{I_a \text{ AMK}}}{\frac{\tau \text{ Prototype}}{I_a \text{ Prototype}}} \quad (2.3)$$

Since the torque produced by the motor is the we get:

$$\frac{K_t \text{ AMK}}{K_t \text{ Prototype}} = \frac{I_a \text{ AMK}}{I_a \text{ Prototype}} \quad (2.4)$$

The torque constant of the *AMK* is provided by the datasheet [5]: $K_t = 0,26 \frac{Nm}{A_{rms}}$, assuming that the motor has yet to lost its properties, we can estimate the prototype K_t :

Speed (rpm)	I rms (A) AMK	I rms (A) Prototype	Kt Prototype
250	3,18	5,13	0,16
500	5	9,87	0,13
750	6,29	13,85	0,12
1250	7,3	19,03	0,10
1500	7,29	20,46	0,09
1750	7,08	21,55	0,09
2000	6,98	22,42	0,08
2250	6,8	22,99	0,08
2500	6,6	23,5	0,07

Table 2.3 - Shor-circuit test raw data

Like at the previous test, we can check suturing happening after 1500 *rpm*, further increasing the *AMK* speed was useless and just kept heating the prototype, the current values showed that the material saturated. If the prototype saturates around 1750 *rpm* and with a current of 21,55A, the K_t is estimated $K_t = 0,09 \frac{Nm}{A_{rms}}$. The maximum torque the motor can achieve is $\tau_m = 1,94 Nm$.

2.3.6 Loaded test

The quadrature inductance L_d parameter is a function of the rotor position due to saliencies. It can be calculated by applying step voltages on V_d and V_q (in open-loop no current control) under locked rotor conditions. It can also be experimentally by finding the quadrature reactance X_d .

$$L_d = \frac{X_d}{2\pi f} \quad (2.5)$$

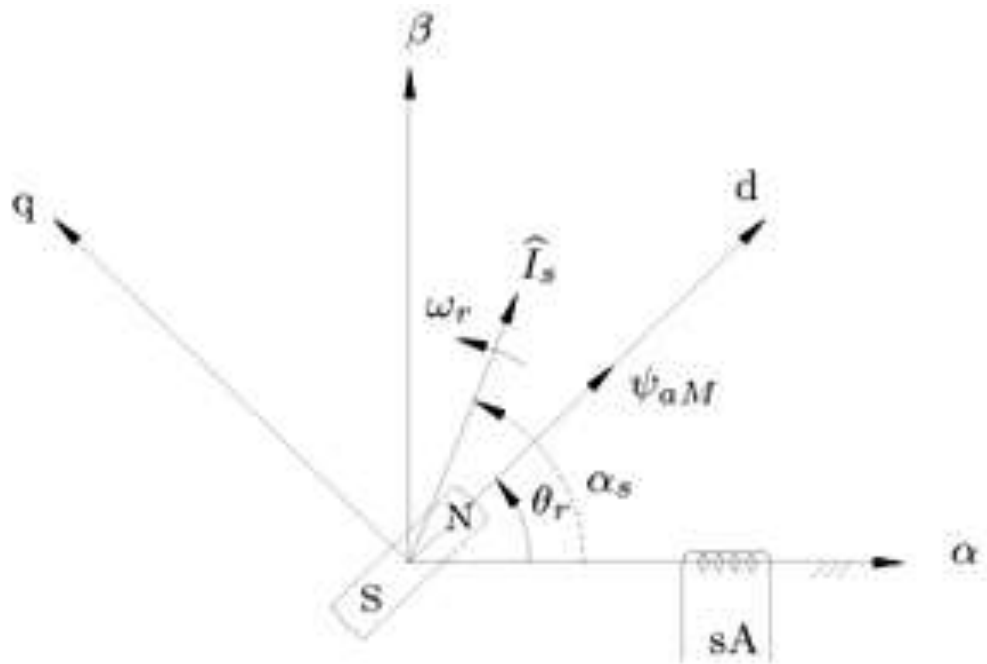


Figure 2.19 - Spatial vectors and magnet flux

f (Hz)	Speed (rpm)	Uab (V)	Ubc (V)	Uca (V)	Ia (A)	Ib (A)	Ic (A)	Ea (V)	Eb (V)	Ec (V)
66,7	1000	8,29	8,29	8,32	0,444	0,431	0,433	4,76	4,75	4,77
133,3	2000	16,95	17,03	17,14	1,497	1,467	1,453	9,51	9,51	9,54
200,0	3000	26,3	26,41	26,52	2,375	2,396	2,389	14,26	14,26	14,32
266,7	4000	34,88	34,97	35,12	2,23	2,236	2,218	19,00	19,01	19,08
300,0	4500	46,8	46,6	48	8,55	8,111	8,222	21,35	21,36	21,44
333,3	5000	54,3	54,1	56,1	10,44	9,82	10,09	23,61	23,61	23,73
366,7	5500	59,9	59,4	61,3	10,3	9,771	9,8	25,92	25,92	26,04
400,0	6000	66,6	67	67,6	10,82	11,05	10,85	28,23	28,23	28,41
433,3	6500	72,3	72,8	73,5	10,98	11,17	10,98	30,60	30,54	30,72

Table 2.4 – Loaded test raw data

Combining this data with the no load test, we can compute X_d :

$$X_d = \frac{\frac{U_{ij}}{\sqrt{3}} - E_i}{I_i} \quad (2.6)$$

Resulting:

Xd			Ld's		
Xa (Ohm)	Xb (Ohm)	Xc (Ohm)	La (H)	Lb (H)	Lc (H)
0,07	0,08	0,08	0,000155	0,000192	0,000191
0,19	0,22	0,24	0,000221	0,000263	0,000289
0,39	0,41	0,42	0,00031	0,000328	0,000331
0,51	0,53	0,54	0,000304	0,000316	0,000322
0,66	0,68	0,76	0,000352	0,000363	0,000405
0,74	0,78	0,86	0,000354	0,000371	0,00041
0,84	0,86	0,95	0,000365	0,000372	0,000414
0,94	0,95	0,98	0,000376	0,000376	0,00039
1,01	1,03	1,07	0,000373	0,000378	0,000392

Table 2.5 - Xd and Ld calculations

Estimated $Ld = 0,354 \text{ mH}$. The set-up for this test can be seen at Figure 2.20.



Figure 2.20 - Test-bench: capacitors, measuring devices and power supply

2.3.7 Saturation Problem Testing

It was very important to find out what was causing the saturation problem, because until now, the prototype was underperforming in every characteristic determined experimentally when compared to the theoretical ones. While some deviation was expected, it would never be of this magnitude.

The first step was to check the quality of the PM, using a gaussmeter, the flux density created by the PM was measured, obtaining a value of $1,4T$ which was the value indicated at the that sheet – the PM were fine.

The next step was to test the rotor material. To do it, using the remains of the stator sheets, a small transformer was built. The rms voltage induced in a transformer is given by

$$E = 4,44\Phi_m f N \quad (2.7)$$

Where ϕ_m is maximum value of the flux in the core, f is operation frequency and N is the number of turns in the coil. The flux in the coil is given by:

$$\phi_m = B_m A_c \quad (2.8)$$

Where, B_m is maximum value flux density in the transformer core and A_c is the cross-sectional area of the core, getting:

$$E = 4,44 B_m A_c f N \quad (2.9)$$

From Biot-Savart's law, is known that a current carrying conductor produces magnetic field and from Ampere's Circuital law, it can be proved that H is proportional to current I . If a current carrying coil produces magnetic flux which traverses an average length of l in complete flux path, then:

$$Hl = NI \quad (2.10)$$

But B and H cannot be measured directly. Having a transformer only allows measures at the terminals, it's required to process the signals. From Faraday's law:

$$V = N \frac{d\phi}{dt} \quad (2.11)$$

Also, from equation (2.6), B is directly proportional to ϕ . A signal proportional to B can be obtained by integrating the voltage signal. The voltage signal can be integrated approximately by using an RC circuit. The transfer function of the circuit is given by:

$$\frac{V_c(s)}{V_{in}(s)} = G(s) = \frac{1}{1 + s\tau} \quad (2.12)$$

Equation (2.8) tells that H is proportional to current. The two signals can be given to two channels of a digital storage oscilloscope. B-H curve of the material can be seen by plotting using *Lissajous*¹ plot settings of the oscilloscope.

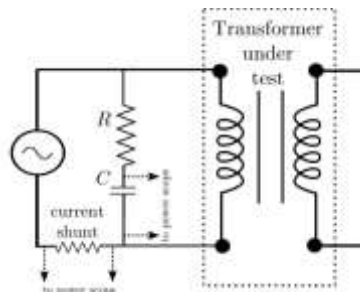


Figure 2.21 - Diagram of the circuit to trace B-H curve measurement

¹ In *Lissajous* plot the signals from two channels are plotted against each other. Otherwise, each signal is plotted against time.

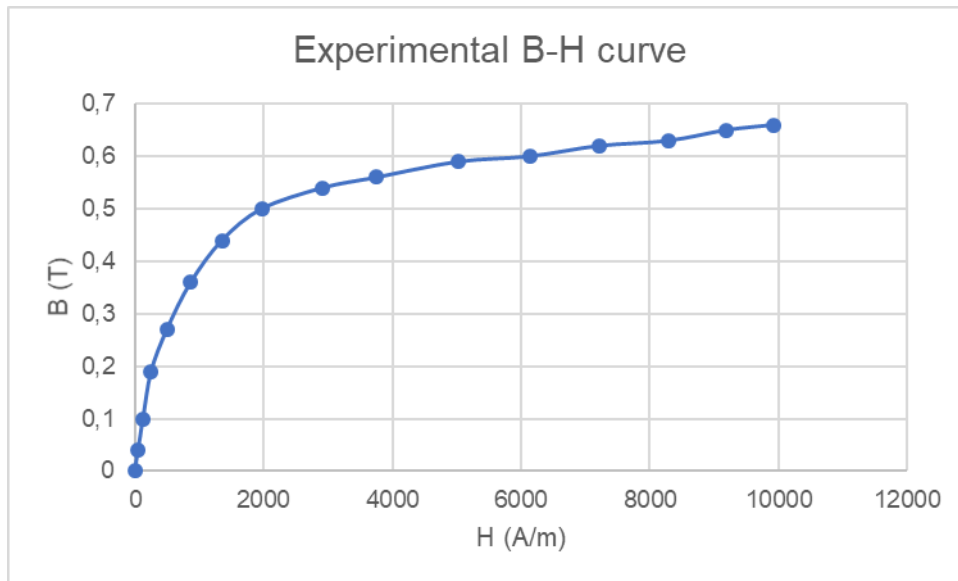


Figure 2.22 - Experimental determination of B-H curve for Vacodur 49

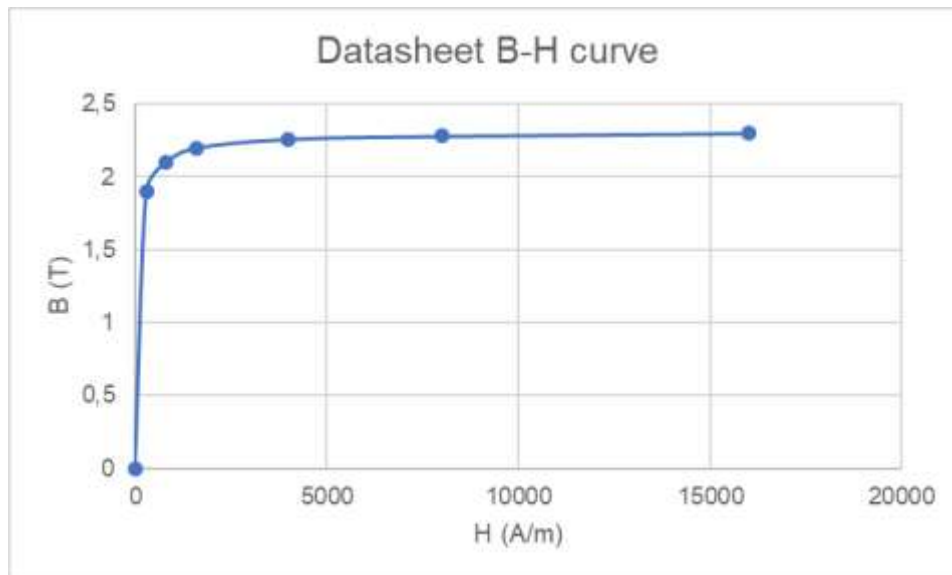


Figure 2.23 - Theoretical B-H curve for Vacodur 49 [8]

The magnet field that the material used in the rotor and stator could create was way too low (seen comparing Figures 2.22 and 2.23). After contacting the seller, it was found out that the shipped material didn't went through a final magnetic annealing process to ensure the properties listed on the data sheet. This problem was unsolvable in this prototype, the temperature used in the annealing are over 750°C and since the magnets could not be removed from the rotor or the coils from the stator, this would ruin it. Also, the epoxy used for the stacking would also fail at that temperature.

2.3.8 Cooling

The coils have a temperature sensor installed which was being checked with a multimeter, while running the no-loads test the temperature would rise slowly up to 60°C . By safety and without cooling, that was the temperature limit set for the tests.

With the cooling circuit on, the temperature was never above 45°C, but the tests were very limited. Due to the saturation of the magnetic steel and the limit of 25A of the cabling used to connect measuring devices, the most power that the high voltage supply fed the motor was 2kW. These results are not representative of real life conditions of the motor.

To test the integrity of this design the circuit was left running for larger minutes to check for possible leaks. Partially blocking the circuit while running to increase the pressure and force leaks on expected weak spots was also tried. No problem was found.

2.4 Testing conclusions

Additional tests like maximum mechanical power, efficiency and endurance testing would be next steps, but due to the previous pointed problems, they're unable to perform. Regarding this, important conclusions were drawn from the tests:

- Parts made of stacking metal sheets in epoxy cannot be cooled down for inference fits.
- The height from the highest point in a coil to the top of the motor housing was too big (5mm), reducing this margin can allow significant weight reduction.
- The winding process must be performed before the stator insertion for reducing the coils height.
- Performing the VPI performance was not possible but given its importance a solution should be arranged.
- There was too much space in the cavity for the encoder, the datasheet suggested the usage of an extra part to secure it against the housing, but it only need to be screwed to the top lid of the motor.
- The *Vacodur 49* need the magnetic final annealing and to insert the epoxy layer with the right thickness before cutting the final geometries.
- The position of the water circuit entrance and exit must be reviewed – the *CAD* model inserted in the car showed no interference, but in real life due to differences in the car, the water fittings were interfering with suspension parts.
- The “one piece” cooling and stator housing works but needs improvements regarding the water circuit.
- The test-bench is working but despite its versatility, it was limited for testing a motor without the problems found in the prototype. It needs improvements: custom made wiring harness – longer and able to withstand the same currents as the car; add a torque sensor; improve overall safety of equipment;

3 Design Process

3.1 Introduction

Developing an electric motor is a complex task, involving disciplines such as electromagnetics, mechanics, thermal, material science, electronics, tribology and mathematics. The design process involves a variety of theoretical analysis, simulations and tests. An optimum design is hard to achieve because every criterion must be comprehensively considered.

There are two basic approaches: a subsystem/component approach and a system approach. While there're differences between the two, they're not opposite, under some circumstances engineering design can gainfully employ both. The first approach consists in breaking down the system to smaller subsystems (rotor, stator, cooling, etc.), design and optimize these subsystems, and then assemble them as the complete system. This approach benefits from simplified problems and shorter design time but ignores interactions among different subsystems.

The system approach focusses on the overall system performance, creating a technical solution that satisfies the system function requirements. It takes account of the intrinsic connections and interactions among different subsystems. The entire system is evaluated to determine how end-use requirements can be provided the most effectively and efficiently. It's based on a top-down strategy, in which the requirements are always satisfied at every step of the process.

The design process starts with the reviewing specifications and requirements, especially the requirements of motor operation and performance. Based on this information, the motor type and topology can be determined, such as PMM or IM, synchronous or asynchronous motor. Then, the main motor design parameters are primarily. The overall sizing of the machine is of great importance in terms of performance, structural integrity, cost, and weight. The major motor dimensions are determined via sizing equations available in the literature. At Figure 3.1 different aspects involving the design of a motor can be found. The literature also suggests how to implement the design process (Figure 3.2).

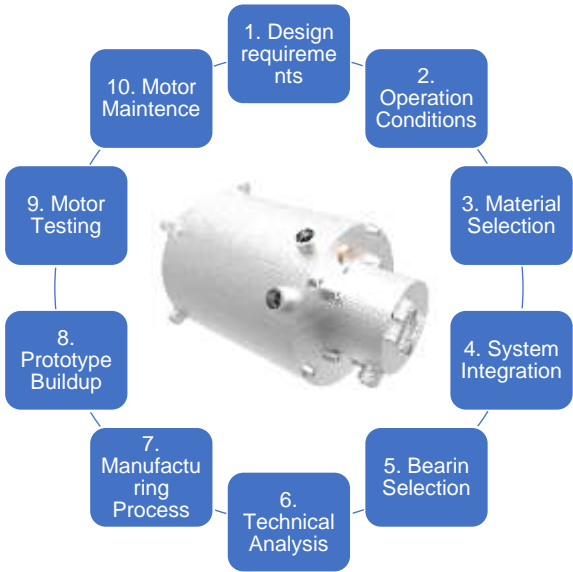


Figure 3.1 - Motor design processes and aspects

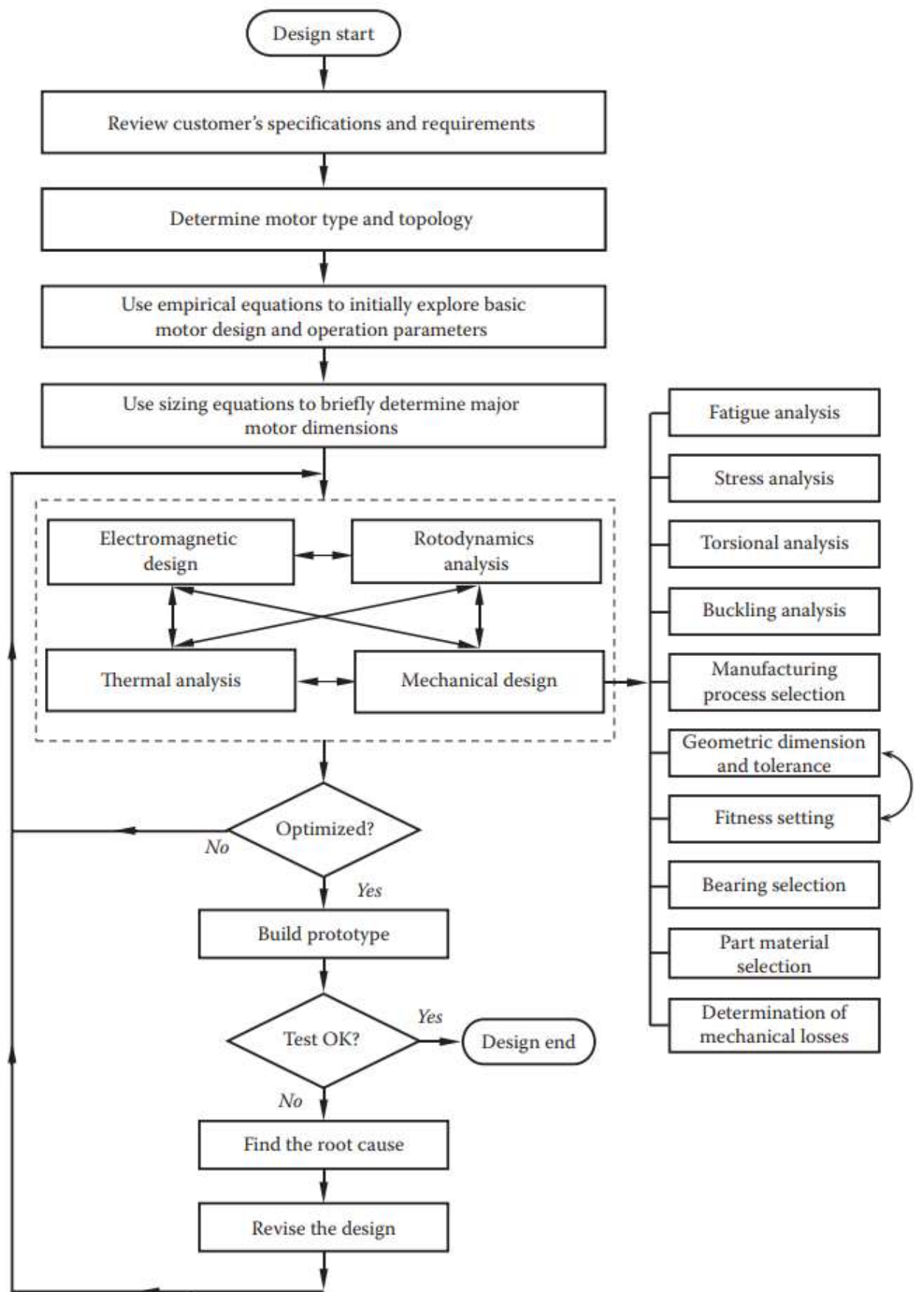


Figure 3.2 - Flow chart of motor design [7]

3.2 Specifications and requirements

The new motor prototype needs to have similar characteristics to the *AMK* motor current in use and be completely compatible with the *AMK* kit inverters (Table 3.1)

Performance data	Stall torque	13,8 Nm
	Maximum torque	21 Nm
	Rated torque	9,8 Nm
	Rated Power	12,3 kW
	Rated Speed	12000 rpm
	Theoretical no-load-speed	18617 rpm
Electrical data	Rated voltage	350 V
	Rated current	41 Arms
	Stall current	53,1 Arms
	Maximum current	100 Arms
	Duration of max current	1,24s
	Torque Constant K_t	0,26 Nm/Arms
	Voltage Constant K_e	18,8 V/krpm
	Rotor time constant	0,01 s
Mechanical data	Motor mass	3,55 kg
	Inertia	2,74 kgcm ²
	Mechanical speed limit	20000 rpm

Table 3.1 - *AMK DD5-14-10-POW - 18600-B5 specs [5]*

Since there's the need to test the motor in the car in parallel with other *AMK* motors, the new one is required to have similar external measures (Figure 3.4) to cause no interference with any other part on the wheel travel. It also needs compatible mounting. To complete the assembly in the car, the *AMK* motor needs an external cooling housing (Figure 3.3). In FST07 and 08e this part was built using a 3D printing process. Made of Alumide, the component weighted 43 *g*. To attach the housing and the motor to the upright is used a front plate made of Al7075, weighting 57 *g*. Taking account, the retainers, O-rings, fittings and silicon to cover leaks, the total assembly of the motor weights 4kg.



Figure 3.3 - Independent cooling housing

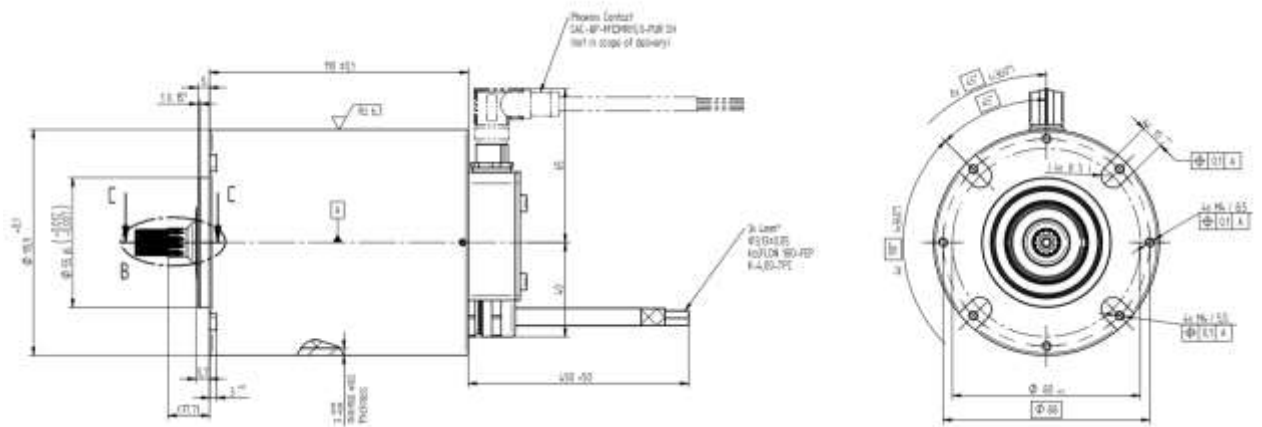


Figure 3.4 - AMK motor dimensions [5]

Only processes affordable or available in the form of sponsorship for the team will be considered and every motor component must comply with the Formula Student Germany rules, *Rules 2019* [6].

It's also required to solve problems found with the interaction between the *AMK* assembly and the car wheel - possible water (cooling) or oil (transmission) leakage. The problems found with the prototype must be addressed too.

Regarding materials, there's the limitation on stator and rotor: the team has already acquired *Vacodur 49* – a cobalt-iron alloy (49% Co - 2% V - Fe Balance - Nb (present) / ASTM A801 Alloy Type 1) with excellent magnetic properties suited for this type of motor [8], already used in the second generation, but this time with the problems fixed.

There's one other material limitation, the PM used will be Neodymium magnets N40 grade with the following dimension $14 \times 5 \times 80 \text{ mm}$. These magnets have a temperature limit of 80°C before start demagnetizing [9] and works until a maximum of 120°C , so this corresponds to the maximum temperature that the rotor can withstand.

As mention before, the motor type will be PMSM with a spoke topology with the restrictions presented at Table 3.2.

Consideration	Requirement	Notes
Motor housing external diameter	95,9 mm	Figure 3.3
Max. Stator external diameter	89,9 mm	Due to Rule XX
Rotor external diameter	60 mm	
Rotor internal diameter	20	
Magnets dimensions	$14 \times 5 \times 80 \text{ mm}$	
Max. stack lengths	80 mm	Due to magnets size
Cooling housing external diameter	110 mm	FST 07 cooling housing

PM max temperature	120°C	
Copper winding temperature	180°C	

Table 3.2 - Geometrical and temperature requirements

Since the propose of this thesis isn't to optimize the winding, this is also a pre-defined requirement, being the same Number of poles – 8 and the same Number of Slots – 24 used in the previous prototypes.

3.3 Concepts

All these constraints lead to different concepts and CAD models. After analyzing its viability and manufacturing, the original concepts were reduced to a few worthy of analysis regarding two subassemblies. The best solution out of both sub-assemblies of the motor will come out after the analysis presented on the next chapters.

3.3.1 Stator, Rotor and shaft

3.3.1.1 Concept 1

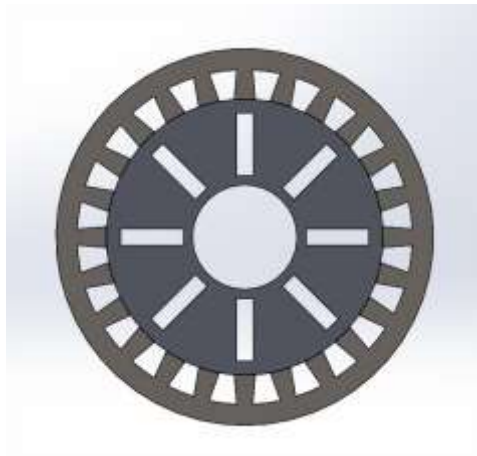


Figure 3.5 - Concept 1 stator and rotor representation

This concept (Figure 3.6) is inspired by PMSM with surface mounted PM, its manufacturing is simple and requires an interference fit that can withstand the motor torque without the shaft slipping inside the rotor. This type of interference can result in losses on the magnetic properties of *Vacodur 49*.

3.3.1.2 Concept 2

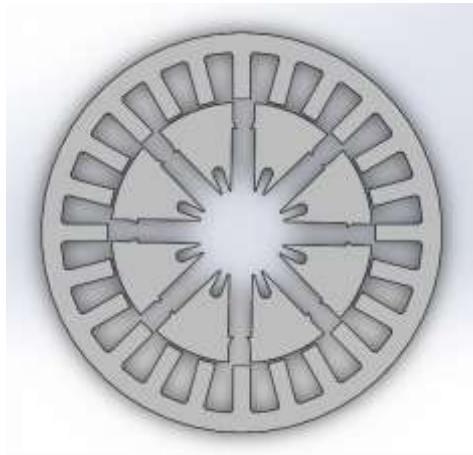


Figure 3.6 - Concept 2 stator and rotor representation

This solution (Figure 3.7) has increased machining difficulty for both shaft and rotor as well as assembling. Since the shaft thins will transmit the forces, the worry of the shaft slipping is no longer present and allows to use an interference fit that only holds the rotor in place relatively to the shaft. Also, in this solution it's possible to see the rotor divided in eight single pieces, but every concept will be study with a full bridge (Figure 3.6), partial bridge (Figure 3.7) or no bridge at all above the magnets, to check the influence on the motor parameters.

3.3.1.3 Concept 3



Figure 3.7 - Concept 3 stator and rotor representation

Contrasting with the previous case, the shaft in this solution (Figure 3.8) is composed by ten parts: a central component with a circular base with rotor radius and a vertical rod where the rotor will slide, eight smaller to align the rotor and a top lid crossed by the smaller rods, above which they will be secured with nuts. This solution can transmit the forces by the smaller rod or due to friction depending on the tightness of the assembly. All parts need a tight fit, but no interference between components.

3.3.1.4 Concept 4

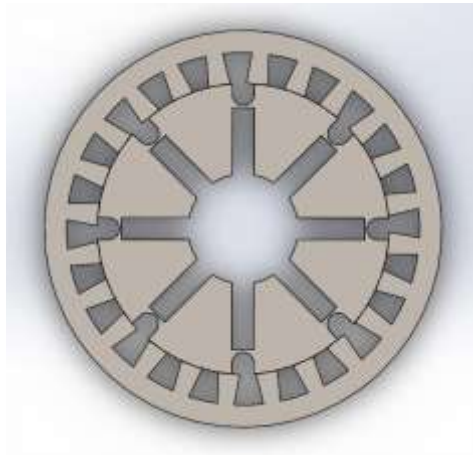


Figure 3.8 - Concept 4 stator and rotor representation

This option (Figure 3.9) is like previous one, but the rods to hold the rotor are above the magnets, causing no interference with the rotor geometry in between magnets. Again, all parts need tight fit, but no interference between components.

3.3.2 **Motor and cooling housing**

3.3.2.1 Concept 5



Figure 3.9 - Concept 5 Chicane circuit

This concept is the current solution used in *FST Lisboa* car: an independent 3D printed cooling housing with chicane like channels perpendicular to the motor Z-axis. The solution delivers and can maintain the motors in their temperature limits, unless extremes conditions occurs. But this solution has a few problems associated: 3D printed plastics sometimes leaves a few pores that, when the water circuit is running looks like a person sweating, the water leakage can cause disqualification in competition; O-rings placing and effectiveness is reduced; easily deformable when mounting on the upright, deformation that creates small crack which leaks water.

3.3.2.2 Concept 6



Figure 3.10 - Concept 6 Spiral circuit

A spiral circuit can be obtained without resorting to 3D printed parts, the spiral can be machined in the motor housing and with an external tube with proper O-rings, the circuit can be completed. This solution can solve a few problems mention before but further analysis regarding its effectiveness is required.

3.3.2.3 Concept 7



Figure 3.11 - Concept 7 Serpent circuit and water representation

The solution was conceived to try to achieve a viable solution for both cooling and motor housing combined, using traditional manufacturing processes. Metal 3D printing would allow this easily, but it's not affordable to the team, maybe in the future with the developing of this type of technologies in national industry, this can become a solution.

4 Electromagnetic analysis

4.1 Finite Element Analysis

4.1.1 Geometry

The geometry is imported from a *CAD* software in 2 dimensions, since the parts to be studied consists on sheets to be stacked, the software used for the analysis allows to make approximations to 3D.

4.1.2 Material properties

Materials are defined for each domain:

- Stator and Rotor – *Vacodur 49*
The B-H curve was presented at Figure 4.1
- Electrical conductivity $\sigma_e = 2500000S/m$
- PM – *NdFeB* magnets air – relative permeability equals to 1,05, relative primitivity equals to one with an electrical conductivity of zero. The B-H curve of the magnets is pre-defined at the materials database of the *FEA* software.
- All other domains like shaft, airgap and outside the rotor are defined as air – relative permeability and relative primitivity equals to one with an electrical conductivity of zero.

4.1.3 Boundary Conditions

The boundary conditions are defined for each domain: i) magnetic insulation set for the outer diameter of the stator; ii) initial value of 0 *Wb/m* applied to all the domains; iii) stator and rotor core are selected with a constitutive relation defined by its B-H curve; iv) PM with a constitutive relation defined by the remnant magnetic flux density, perpendicular to the magnet radial axis, with 1.3 *T* and with the same magnetic poles facing two consecutive magnets; v) the coils domains are selected having a sinusoidal external current density with an amplitude of $10A/mm^2$ with a phase difference of one third the period between each phase and with a frequency of 400Hz. The current density was defined taking into consideration that $10A/mm^2$ is the boundary between a highly efficient heat removal fan cooling system and a non-efficient heat removal liquid cooled system (that can increase to $30A/mm^2$ for highly efficient systems) [12]. Once the cooling system had never been developed and tested before, a conservative value for the current density was chosen. 400Hz was defined based on the average speed the car does (which is proportional to motor speed), during an endurance race.

4.1.4 Mesh

Mesh quality has great importance to perform finite element analysis, but better mesh comes with the cost of higher computational costs. It's important to find a balance. In the analysis to be performed, to start it will be used the standard meshes and keep refining it until a convergence is found.

4.1.5 Simulation

A parametric study will be used to estimate the maximum motor torque. In this study the angle of the magnetic flux created by coils inside the stator slots rotate while the rotor and PM are fixed. The *FEA* software solves the Maxwell equations [13]. To compute torque, it will be used the Maxwell Stress Tensor (MST): by integrating the MST along a surface it's possible to obtain the force. The method is

simple and requires little simulation time, despite the possibility of being less accurate. For two dimensional models the relation is:

$$T_e = \frac{L}{\mu_0} \int_0^{2\pi} r^2 B_r B_\theta d\theta \quad (4.1)$$

T_e is the electromagnetic torque, L the active length of the machine, r the radius of closed surface at the motor airgap, B_r and B_θ are the radial and tangential components of the flux density. The result is multiplied by the number of pole pairs.

Applying the MST method with the FEA software, the equation used is [13]:

$$n_1 T_e = -\frac{1}{2} n_1 (H \cdot B) + (n_1 \cdot B) B^T \quad (4.2)$$

By integrating it on the surface to obtain the force where n_1 is the outward from the object, T_e is the torque, E is the electric field, D the electric displacement, H the magnetic field, B the magnetic flux density. There are more accurate methods, it is easier to define when programing the FEA software since it's available in the software used.

4.2 Results

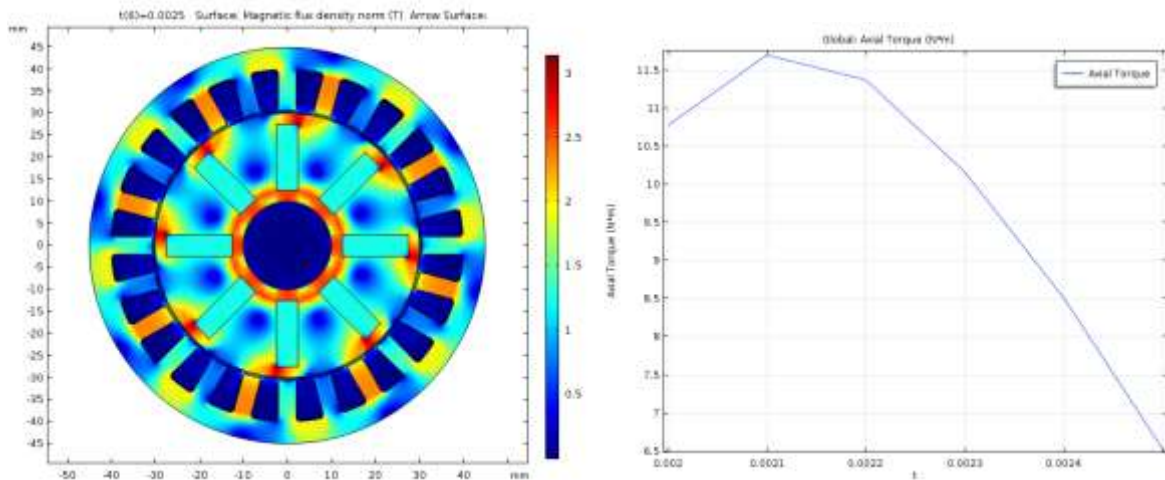


Figure 4.1 - Magnetic Flux density (left) and Axial torque (right) for concept 1

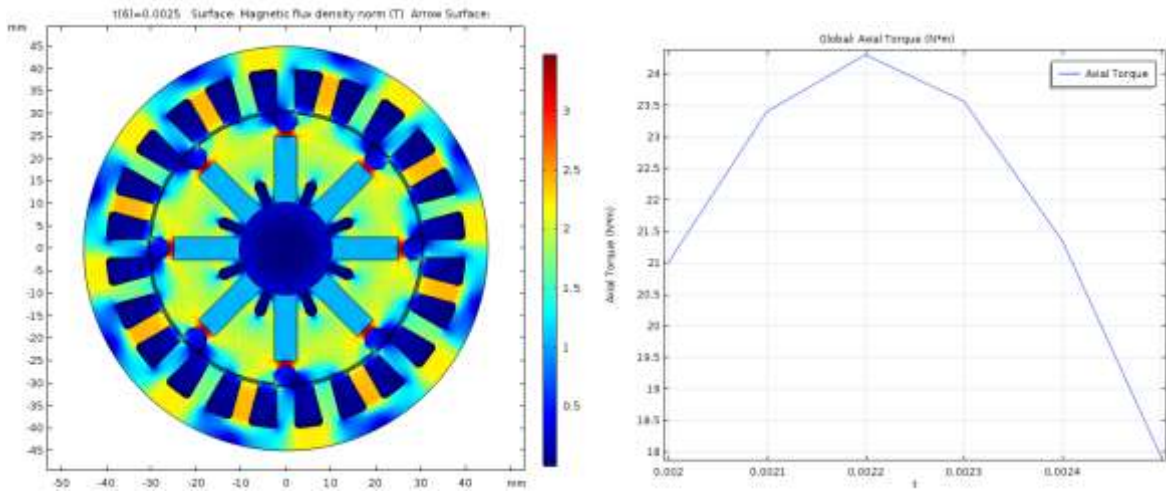


Figure 4.2 - Magnetic Flux density (left) and Axial torque (right) for concept 2

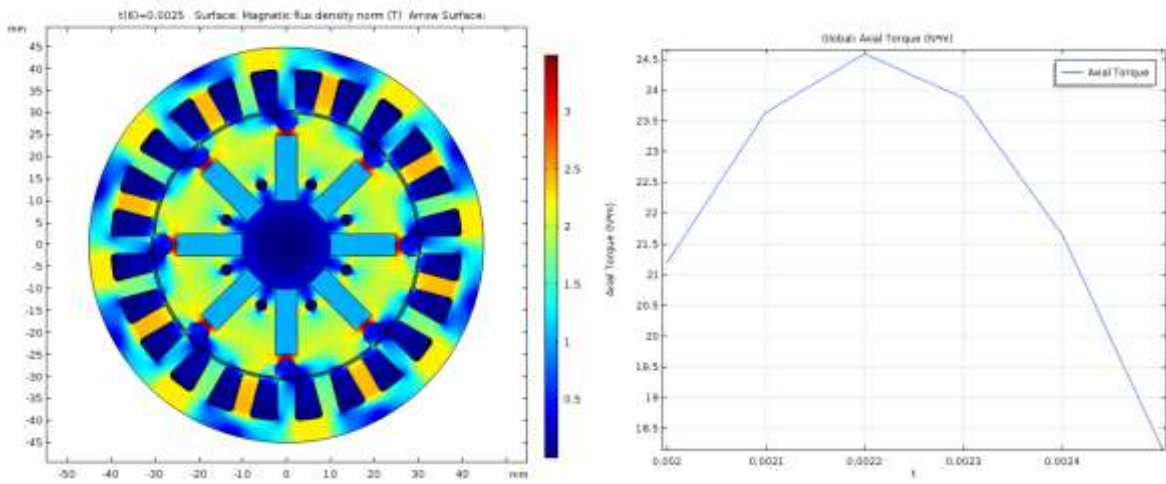


Figure 4.3 - Magnetic Flux density (left) and Axial torque (right) for concept 3

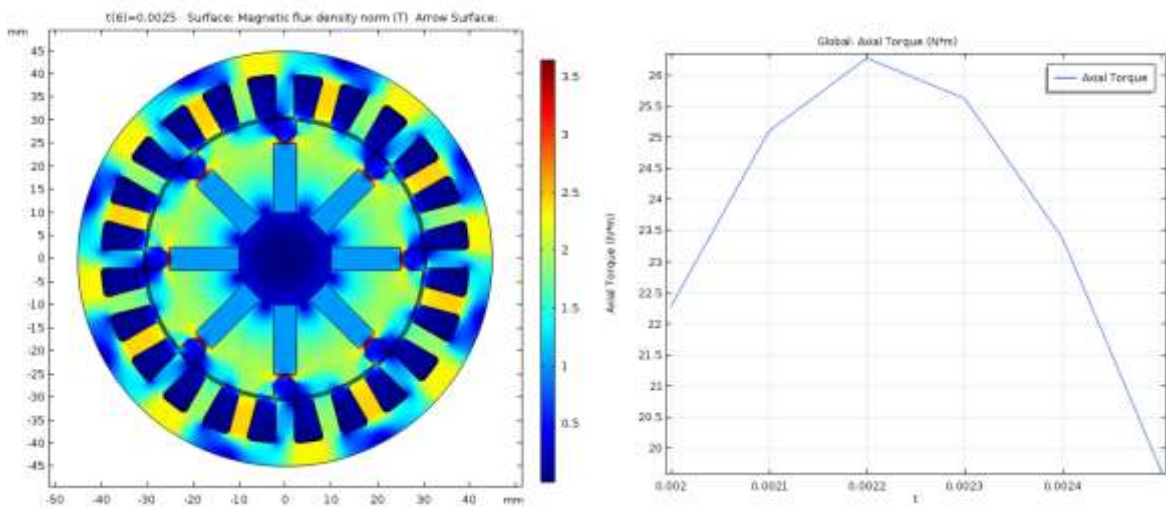


Figure 4.4 - Magnetic Flux density (left) and Axial torque (right) for concept 4

Concept	Max. Torque (Nm)
1	11,7
2	24,3
3	24,5
4	26,2

Table 4.1 - Estimated maximum torque results

After analyzing Figures 4.1 to 4.4, the solution chosen for further iteration is concept 4, this solution offers a higher torque and it's simpler compared to concepts 2 and 3. Concept 1 doesn't offer any advantage.

5 Thermal analysis

5.1 Finite Element Analysis

5.1.1 Geometry

The geometry is imported from a CAD software in three dimensions: this includes a model from the rotor, stator, magnets, housing, shaft, air inside the motor and water from the cooling circuit.

5.1.2 Material properties

Materials (Table 5.1) are defined for each domain:

Domain	Material	Heat Capacity C_m (J / K mol)	Thermal Conductivity c_s ($\frac{W}{m.K}$)
Stator and Rotor	Vacodur 49	-	29,8
Coils	Copper	0,385	385
Cooling fluid	Water	4,178	0,0187
Housing	AL7075	0,96	130

Table 5.1 - Domains and Material for thermal simulation

Due to regulation only water, air or mineral oil can be used as cooling fluids. Since air cooling isn't enough to keep the motors at the correct temperature and using oil would escalate the complexity of the car cooling system, water is the one to use-

5.1.3 Boundary Conditions

A steady state regime will be considered for faster results and less computation resources. The simulations will be performed for a situation when the motor is working at its nominal power. This translates in imposing 2200W distributed by the 24 stator slots [5].

A mass flux of water of $0,1 \frac{kg}{s}$ (the pump allows a maximum of $0,282 \frac{kg}{s}$ and 8m of elevation) is imposed at entrance of the circuit. On the wall and non-slipping condition is applied. The heat flux is imposed at the external wall of the stator housing, the other faces are considered isolated.

The outer boundary condition for heat exchange is calculated by the convective heat flux between the engine walls and the air over the various iterations by the program according to:

$$Q = hA(T_s - T_\infty) \quad (5.1)$$

Where h is the convection heat transfer coefficient, A the heat exchanging area, T_s the surface temperature and T_∞ the fluids temperature [14].

5.1.4 Mesh

Like in the electromagnetic analysis, it will be used the standard meshes and keep refining it until a convergence is found. Being a three dimensional model with numerous domains, makes difficult to build goods automatic meshes. Manual corrections are necessary between elements in the domain frontiers.

5.1.5 Simulation

We can model the flow of a fluid using three equations: continuity, energy and momentum conservation. The first refers to the conservation of mass and can be written as:

$$\frac{\partial \rho}{\partial t} + \nabla \cdot (\rho \vec{U}) = 0 \quad (5.2)$$

When integrated into a control volume, the mass flow that is exchanged on the surfaces of that volume must be equal to the mass change in the control volume. For an incompressible fluid the equation is reduced to:

$$\nabla \cdot \vec{U} = 0 \quad (5.3)$$

By applying Newton's second law to the fluid, we can get the equation of momentum conservation:

$$\frac{\partial}{\partial t}(\rho \vec{U}) + \nabla \cdot (\rho \vec{U} \vec{U}) = -\nabla p + \nabla \cdot T \rho \vec{g} + \vec{F} \quad (5.4)$$

On the left side we have the term transient and convective flow, while on the right side correspond, respectively, to the terms of the pressure gradient, p , T is the stress tensor and \vec{F} represents the forces acting on the fluid, per unit volume, which are related to the effects of rotation, thrust and other sources of movement on the fluid.

The stress tensor is given by:

$$T = \mu \left[(\nabla \vec{U} + \nabla \vec{U}^T) - \frac{2}{3} \nabla \cdot \vec{U} Id \right] \quad (5.5)$$

Where μ dynamic viscosity and the second term from the right side represents the volume expansion [14].

Using Gauss's divergence theorem, integrating the previous equation into a control volume V :

$$\partial t \int_V \rho \vec{U} dV + \oint_A \rho \vec{U} \cdot \vec{U} dA = - \oint_A p Id \cdot dA + \oint_A T \cdot dA + \int_V \rho g dV + \int_V F dV \quad (5.6)$$

The energy equation is formulated as:

$$\frac{\partial}{\partial t}(\rho E) + \nabla \cdot (\vec{U}(\rho E + p)) = \nabla \cdot (k_{eff} \nabla T + (\vec{T} \cdot \vec{U})) + S_h \quad (5.7)$$

The first term corresponds to the transient term and the second to the convective. On the right side are represented the term diffusive and those representing the viscous effects and sources, or energy wells. E corresponds to the energy, k_{eff} corresponds to the effective conductivity ($k + kt$) where the latter represents the turbulent thermal conductivity, calculated according to the chosen turbulence

model, ∇T to the temperature gradient, σ as the stress tensor and S_h represents sources, or energy wells.

The FEA software using an iterative method GMRES, can solve the system of linear equations. It's used an iterative method to gradually get closer to solution. Since it's a Multiphysics problem, the equation that describe temperature, speed and pressure are solved individually [15].

5.2 Results

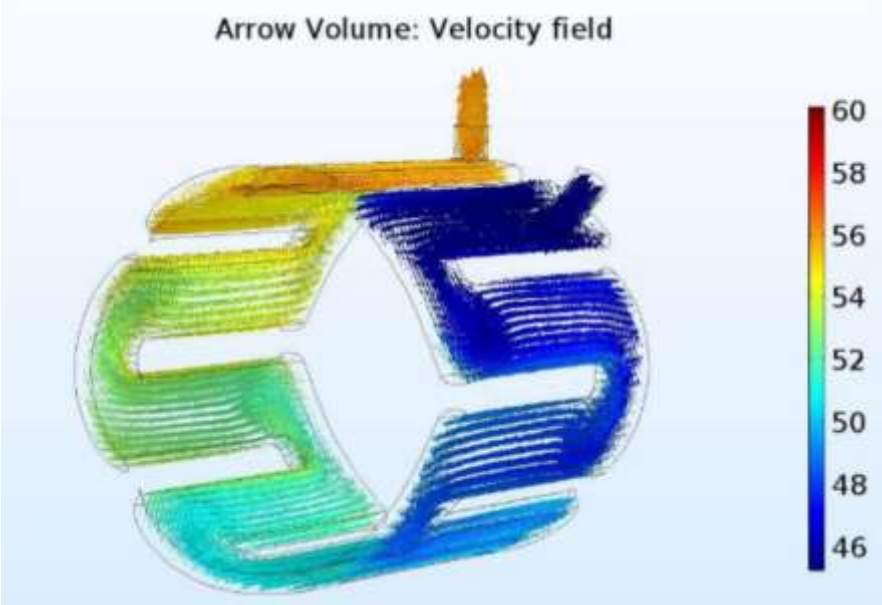


Figure 5.1 - Water circuit Concept 7

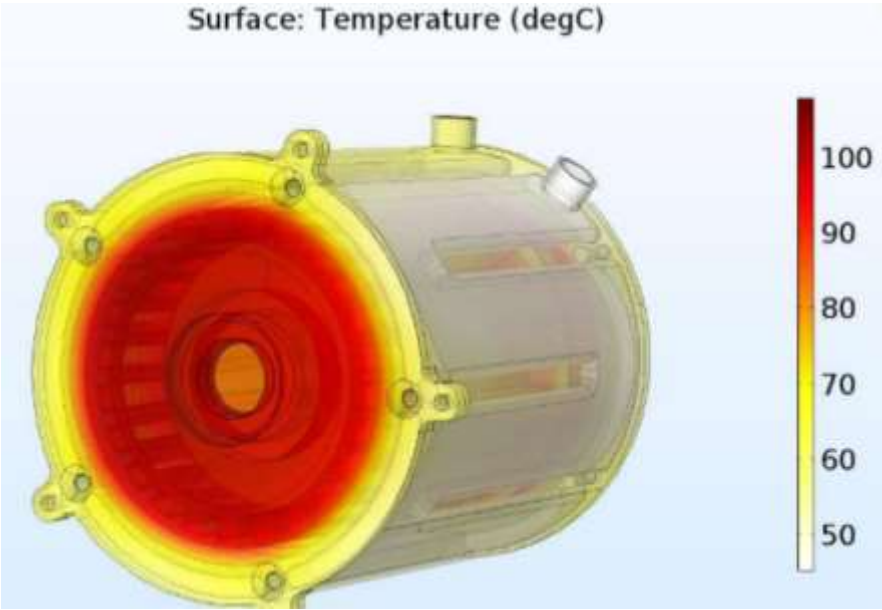


Figure 5.2 - Motor temperatures

Concept	Rotor		Stator		Copper		Water		Losses (mH ₂ O)
	Av (°C)	Max (°C)	Av (°C)	Max (°C)	Av (°C)	Max (°C)	Av (°C)	Max (°C)	
5	72,03	72,44	56,48	82,25	71,13	85,2	42,56	60,51	0,68
6	73,64	73,97	57,35	82,55	73,02	85,49	40,88	65,235	1,72
7	70,57	70,78	63,91	81,01	76,37	87,01	49,17	56,85	3,58

Table 5.2 - Thermal analysis results

All concepts are very similar and it's hard to understand if the difference between each other is so small. All studies were performed under the same conditions, but this simulation had to many domains and the mesh quality was hard to evaluate. But again, the same conditions were applied to all, and it's known that concept 5 works in real life but it's concept 7 that gathers more advantages regarding materials, manufacturing and assembling. Further, when designing the motor housing, a hybrid solution of concept 5 and 7 will be made.

6 Mechanical Design

6.1 Shaft

The shaft to be used with Concept 4, consists in ten individual components: one part that is the base for the rotor, holder for the first bearing and also the connection the transmissions; one part to seat in top of the rotor, holding the second bearing and connect to the encoder and eight equal rods to ensure the rotor right position and to press both top and better part together (Figure 6.1).

The torque produced at the rotor will be transmitted by the shaft to the car transmission by friction. The bottom and top parts need to be tight enough to ensure the torque transition. Regardless, there's a safety mechanism in case the first way of transmitting torque fails, the 4 vertical rods will be dimensioned to withstand the maximum torque. This leaves four aspects to study: i) critical radius of the shaft on the transmission part coupling; ii) the critical diameter of the rods; iii) critical radius for the hollow part of the shaft inside the rotor; iv) Contact pressure for torque transmission by friction.

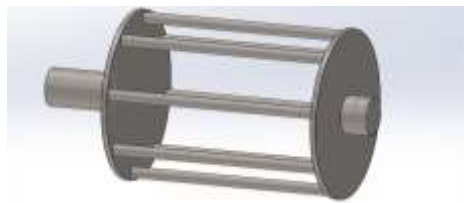


Figure 6.1 - Initial iteration for Concept 4 shaft

Materials

Selecting a proper material for the shaft is critical for ensuring the motor normal and safe operation. The most widely used shaft material is carbon steel, but recently other materials like high tensile aluminum alloys or titanium enhanced aluminum alloys are being considerate. The following materials are considered due to its low price (steel) or their availability to the team:

Material	Yield Tensional Strength (MPa)	Ultimate Tensional Strength (MPa)	Shear Strength (MPa)	Fatigue Strength (MPa)	Hardness Brinell (HB)	Density (g/cm ³)	Strength-density ratio
AISI 1008 cold rolled	285	340	196	170	95	7,872	36,2
AISI 1020 cold rolled	350	420	242	193	121	7,87	44,5
AISI 1045 cold rolled	505	585	338	268	170	7,87	64,2
Ductile iron 65-45-12	310	448	336	179	131-220	7,1-7,2	43,1
A7075-T6	503	572	331	159	150	2,81	179
Ti90/Ai6/V4	880	950	550	240	334	4,43	198,6

Table 6.1 - Shaft material properties [16][17][18][19]

Since keeping low the total weight of the motor, the lower density materials are attractive. Despite not being the lightest material available, the titanium alloy will be chosen due to its higher strength-density ratio. Also, the aluminum alloy is more susceptible to heat expansion than any other material considered, which can be a problem for the rotor.

Shaft critical sections

The theoretical maximum torque the motor can achieve is 26,2 Nm, models often differs from real life results, so it's expected the maximum torque to be lower. In the following analysis, tanking this into account, a minimum of 1 as safety factor will be considered enough, considering a 27 Nm torque.

- i) Shaft critical radius, r_{shaft}

We can compute the shear stress using:

$$\tau = \frac{T_r r_{shaft}}{J_T} \quad (6.1)$$

Where T_r is the applied torque and J_T the torsion constant for the section that ca be obtained by:

$$J_T = \frac{\pi r_{shaft}^4}{2} \quad (6.2)$$

Assuming the shear stress equal to the shear strength of the material and combining (6.1) and (6.2) the critical radius for this section is:

$$r = \sqrt[3]{\frac{T_r}{\frac{\pi}{2} \tau}} = \sqrt[3]{\frac{27 * 1000}{\frac{\pi}{2} * 550}} = 3,15mm \quad (6.3)$$

- ii) Rods critical diameter - d_{bolt}

Basically, this consists about calculating the diameter of the bolted connections.

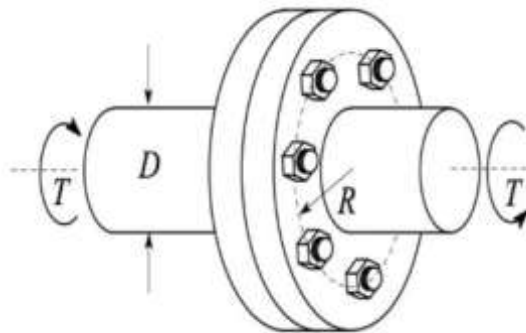


Figure 6.2 - Bolts disposition example

In this case (Figure 6.2), with eight equally spaced and centered with a radius of $R_{bolts} = 56mm$. The torque to apply is $T_r = 27Nm$ and the rotor diameter $d_{rotor} = 60mm$.

The force in the bolt due to torque is:

$$F_t = \frac{T_r}{8R_{bolts}} \quad (6.4)$$

The force in the bolts due to stress is:

$$F_s = \left(\frac{16T_r}{\pi d_{rotor}^3} \right) \left(\frac{\pi}{4} d_{bolt} \right) \quad (6.5)$$

The force due to torque and the force due to stress must be equal in this situation:

$$\frac{T_r}{8R_{bolts}} = \left(\frac{16T_r}{\pi d_{rotor}^3} \right) \left(\frac{\pi}{4} d_{bolt} \right) \quad (6.6)$$

Using the given values, $d_{bolt} = 3mm$. This value is smaller than $4mm$ that is the minimum required according to *FSG Rules 2020 - T 10.1.2* for critical fasteners.

iii) Critical radius for hollow part

In this case, the torsion constant is obtained with:

$$J_T = \frac{\pi}{2} (R_{shaft}^4 - r_{shaft}^4) \quad (6.7)$$

In which R_{shaft} represents the outside diameter of the hollow section and it's equal to the inside diameter of the rotor, $R_{shaft} = 20mm$. Leading to $r_{shaft} = 19,9mm$.

iv) Contact pressure for torque transmission by friction

To be able to transmit torque due to friction, the normal force produced by the bolts must be higher than the force produced by the motor:

$$F_T \leq \mu F_N \quad (6.8)$$

$$F_T = \frac{T}{r_{rotor}} = \frac{27}{0.06} = 450 N \quad (6.9)$$

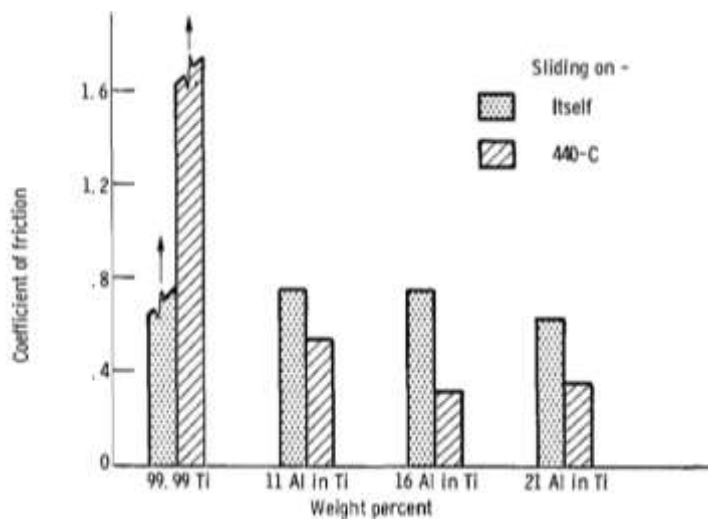


Figure 6.3 - Coefficient of friction and rider wear for titanium and titanium-aluminum alloys sliding on themselves and on 440-C stainless steel [20]

With $T = 27 Nm$, $r_{rotor\ ext} = 60 mm$, $r_{rotor\ int} = 20 mm$, assuming the worst case scenario for the coefficient of friction $\mu = 0,3$ (Figure 6.3), we get $F_N = 1500N$. This force will be distributed by eight bolts that leads to a minimum pre-load per bolt of $F_{pre-load\ per\ bolt} = 187,5N$. A M4 with 8.8 Grade has preload of $4000N$ [21], so it's safe to assume the rotor will not slip and put the rods into a shear situation.

Static failure analysis

When a force is applied to a solid body, it causes a deformation. The work done on the solid, is proportional to the force and deformation. The work done by applied force is stored in the solid as potential energy, which is called the strain energy. The strain energy in the solid may not be distributed uniformly throughout the solid. The concept of strain energy density is strain energy per unit volume - U_0 . Then the strain energy in the body can be obtained by integration as follows[22]:

$$U = \iiint_V U_0(x, y, z) dV \quad (6.10)$$

Where V the body volume. Considering, In the case of uniaxial stress state strain energy density is equal to the area under the stress–strain curve, allowing to write:

$$U_0 = \frac{1}{2} \sigma \varepsilon \quad (6.11)$$

For the general three dimensional, the strain energy can be expressed as:

$$U_0 = \frac{1}{2} \sigma_x \varepsilon_x + \sigma_y \varepsilon_y + \sigma_z \varepsilon_z + \tau_{yz} \gamma_{yz} + \tau_{zx} \gamma_{zx} + \tau_{xy} \gamma_{xy} \quad (6.12)$$

With an elastic material, the strain energy can be completely recovered by unloading the body.

Considering a coordinate system that is parallel to the principle stress directions, the equation (6.12) can be simplified. In this coordinate system no shear component exists:

$$U_0 = \frac{1}{2} \sigma_1 \varepsilon_1 + \sigma_2 \varepsilon_2 + \sigma_3 \varepsilon_3 \quad (6.13)$$

Stresses and strains are related through the linear elastic relations, the principal stresses and strains:

$$\begin{cases} \varepsilon_1 = \frac{1}{E} (\sigma_1 - \nu \sigma_2 - \nu \sigma_3) \\ \varepsilon_2 = \frac{1}{E} (\sigma_2 - \nu \sigma_1 - \nu \sigma_3) \\ \varepsilon_3 = \frac{1}{E} (\sigma_3 - \nu \sigma_1 - \nu \sigma_2) \end{cases} \quad (6.14)$$

Substituting equation (6.14) into (6.13) the strain energy can be density can be written as:

$$U_0 = \frac{1}{2E} [\sigma_1^2 + \sigma_2^2 + \sigma_3^2 - 2\nu(\sigma_1 \sigma_2 + \sigma_2 \sigma_3 + \sigma_3 \sigma_1)] \quad (6.15)$$

The strain energy density can be divided in two parts: i) dilatational strain energy density U_H and ii) distortional strain energy density. The last one is responsible for change in shape.

$$U_d = \frac{1 + \nu}{3E} \frac{\sigma_1 - \sigma_2^2 + \sigma_2 - \sigma_3^2 + \sigma_3 - \sigma_1^2}{2} \quad (6.16)$$

Writing U_d in terms equivalent von Mises stress σ_{VM} :

$$U_d = \frac{1 + \nu}{3E} \sigma_{VM}^2 \quad (6.17)$$

The von Mises stress is defined in terms of principal stresses as:

$$\sigma_{VM} = \sqrt{\frac{\sigma_1 - \sigma_2^2 + \sigma_2 - \sigma_3^2 + \sigma_3 - \sigma_1^2}{2}} \quad (6.18)$$

According to von Mises's failure criterion, a material under multi-axial loading will yield when the distortional energy is equal to or greater than the critical value for the material:

$$\begin{aligned} \frac{1 + \nu}{3E} \sigma_{VM}^2 &\geq \frac{1 + \nu}{3E} \sigma_Y^2 \\ \therefore \sigma_{VM} &\geq \sigma_Y \end{aligned} \quad (6.19)$$

The distortion energy theory can be stated that material yields when the von Mises stress exceeds the yield stress obtained in a uniaxial tensile test. The von mises can be rewritten in terms of stress components as:

$$\sigma_{VM} = \sqrt{\frac{(\sigma_{xx} - \sigma_{yy})^2 + (\sigma_{yy} - \sigma_{zz})^2 + (\sigma_{zz} - \sigma_{xx})^2 + 6(\tau_{xy}^2 + \tau_{yz}^2 + \tau_{zx}^2)}{2}} \quad (6.20)$$

For a two-dimensional plane stress state, the von Mises stress can be defined in terms of principal stresses as:

$$\sigma_{VM} = \sqrt{\sigma_1^2 - \sigma_1 \sigma_2 + \sigma_2^2} \quad (6.21)$$

And in terms of general stress components as

$$\sigma_{VM} = \sqrt{\frac{\sigma_{xx}^2 + \sigma_{yy}^2 - \sigma_{xx} \sigma_{yy} + 3\tau_{xy}^2}{2}} \quad (6.22)$$

This failure criteria will be applied for the static analysis of the motor components and safety factor compute.

The three dimensional model of the shaft will consist on a single component for this studies purpose. This allows lower computation times and simpler meshes. Other changes need to accommodate components not yet presented will not be included in the *FEA* model.

The loads cases for which the shaft is studied are:

- i) a worst scenario of the maximum torque being applied to a blocked transmission - torque of $T_r = 27 Nm$
- ii) bump force on the tire – at the time of a bump, a force will act on the portion of the shaft inside the wheel assembly because the motor is assembled directly to it. This force is obtained from the wheel rate. Assuming a wheel a wheel rate of $45N/mm$ and travel due to bump of $25 mm$: $F_b = 45 * 25 = 1125N$
- iii) weight of the vehicle: assuming a $250 kg$ weight + $70 kg$ pilot with a $50/50$ weight distribution, the force on each wheel is: $F_w = (250 + 70) * \frac{9.81}{4} = 784,8 N$

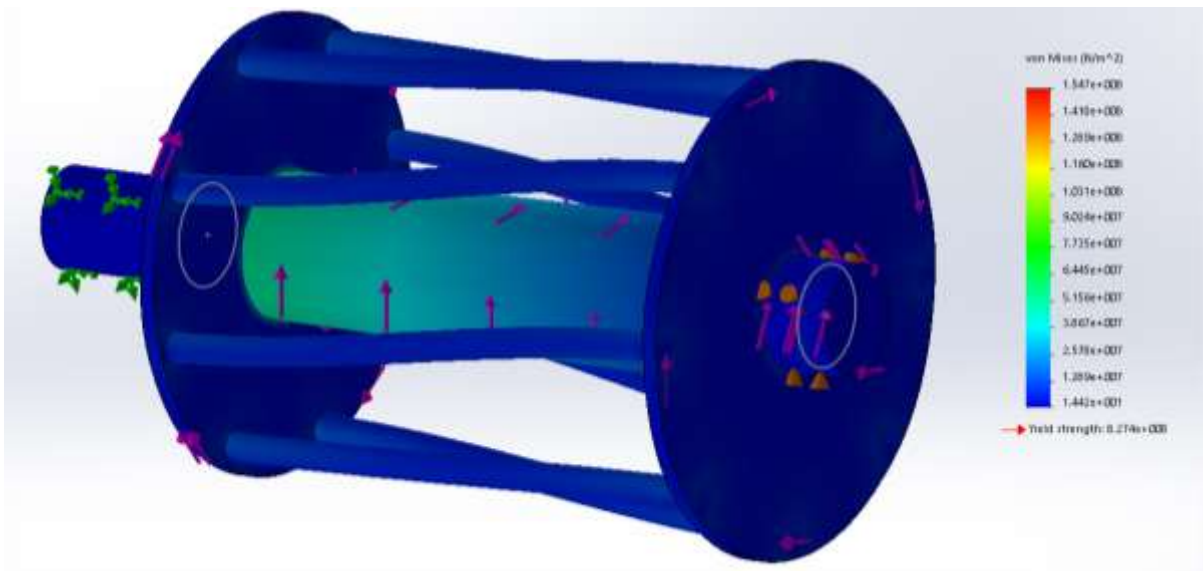


Figure 6.4 - Von Mises stresses on shaft for torsional analysis

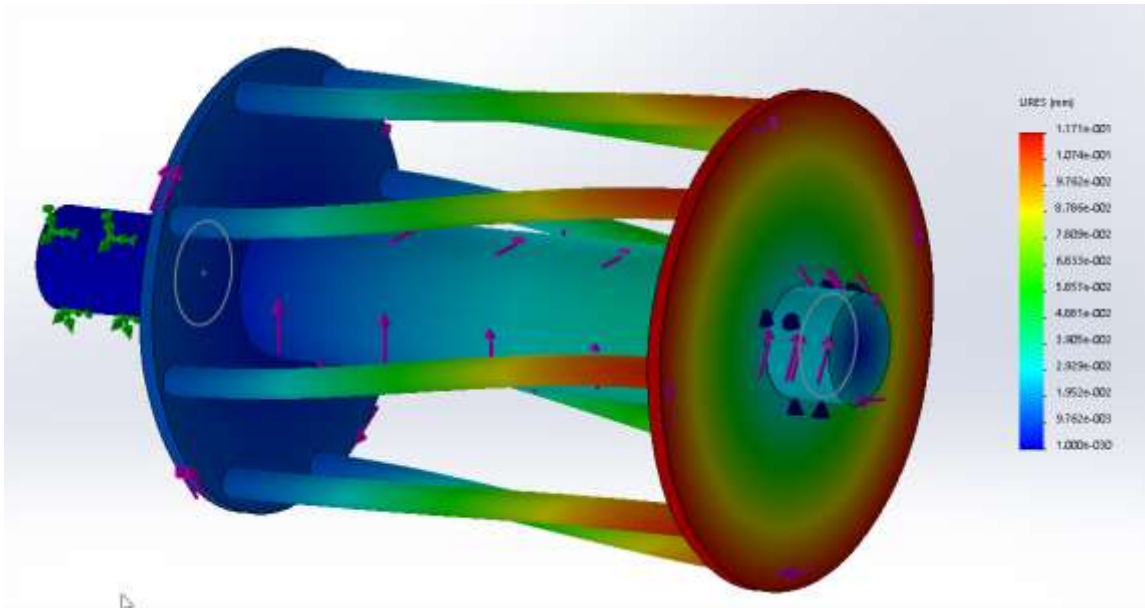


Figure 6.5 - Safety factor for shaft torsional analysis

<u>Load</u>	<u>Max Von Mises (MPa)</u>	<u>Max deformation (mm)</u>	<u>Min Safety Factor</u>
Torsional	154,7	0,117	3
Bump	75,43	0,04	3
Car weight	52,78	0,024	3
All combined	154,8	0,117	3

Table 6.2 - Stress analysis results - shaft

Looking at the results, the shaft is clearly over-dimensioned. But this is a positive aspect to a system with little real-life experience. This can also be justified by the need to comply with the rules. Upon the validation of this motor, less conservative designs can be done to reduce weight.

Shaft key

The AMK motor assembly doesn't have a mechanical fuse. This was one of the causes of a serious accident that happened while testing *FST08e*. One time during a simulation endurance the hub of a wheel broke, caused by a locking of the transmission while the motor kept trying to deliver torque. After analyzing the broken parts, cracks propagated due to fatigue were the failure cause. Sometimes problems like this can happen, but the damage must be kept to a minimum. In order to do this, the shaft will incorporate a key to be used as a fuse.

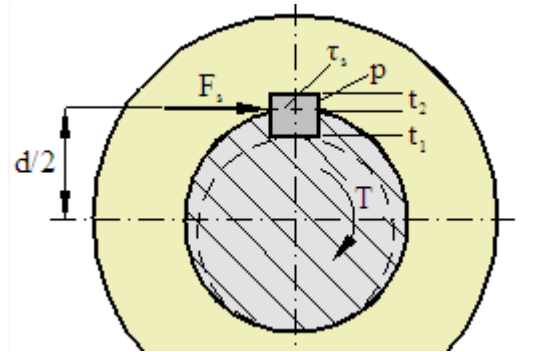


Figure 6.6 - Shaft keys and keyways

Recurring to a key and keyway calculator, knowing the maximum torque and assuming the key length of the key $L = 15mm$ - the key length should be less than about 1.5 times the shaft diameter ($12mm$) to ensure a good load distribution over the entire key length when the shaft becomes twisted when loaded in torsion. We have:

key width b	4mm
key height h	4mm
keyway depth shaft t_1	2.5mm
keyway depth hub t_2	1.8mm

Table 6.3 - Key dimensions

Manufacturing

Contrasting to the second generation prototype, the components of this shaft can be obtained by conventional processes, a conventional mill is enough.

6.2 Rotor

There's no material analysis at this point, *Vacodur 49* was chosen for its magnetic properties and it was a design requirement to use this material.

Static failure analysis

Most rotor dimensions are previous defined, leaving at this stage to confirm only if it withstands the same conditions previous mentioned in the shaft:

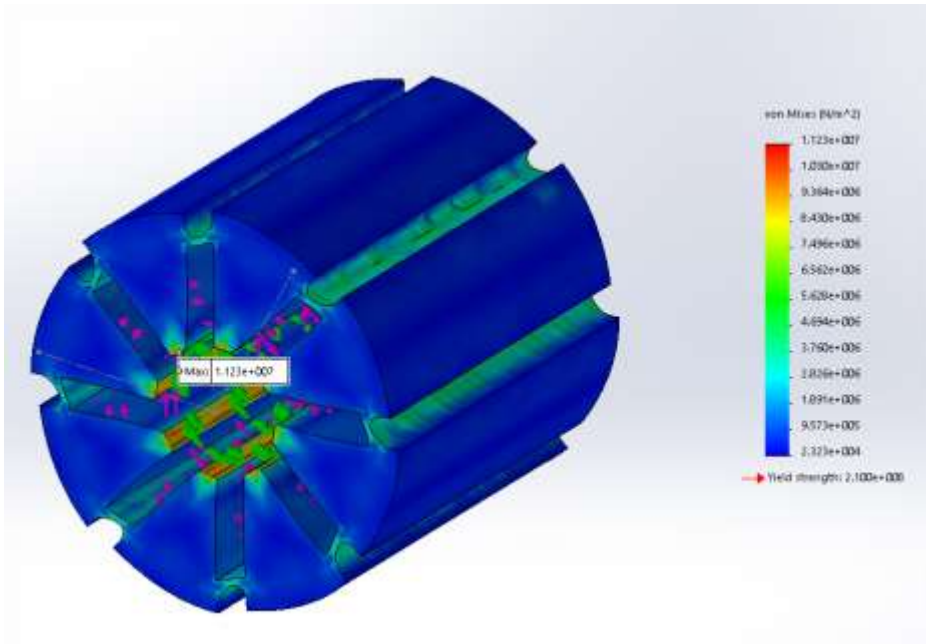


Figure 6.7 - Von Mises stresses on rotor for torsional analysis

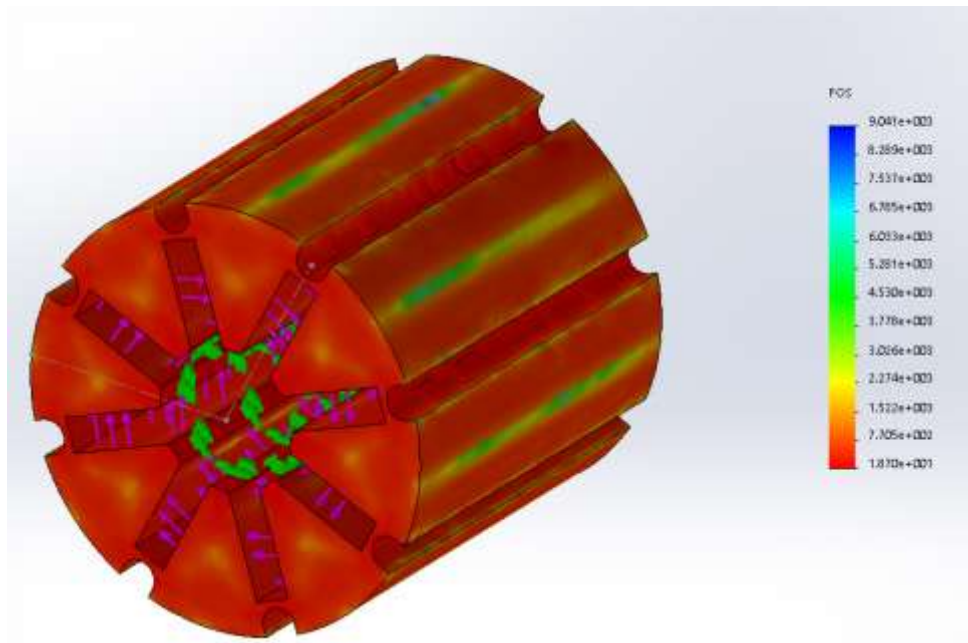


Figure 6.8 - Safety factor for rotor torsional analysis

It's also important to check the centrifugal force at the rotor at maximum speed – 20000rpm:

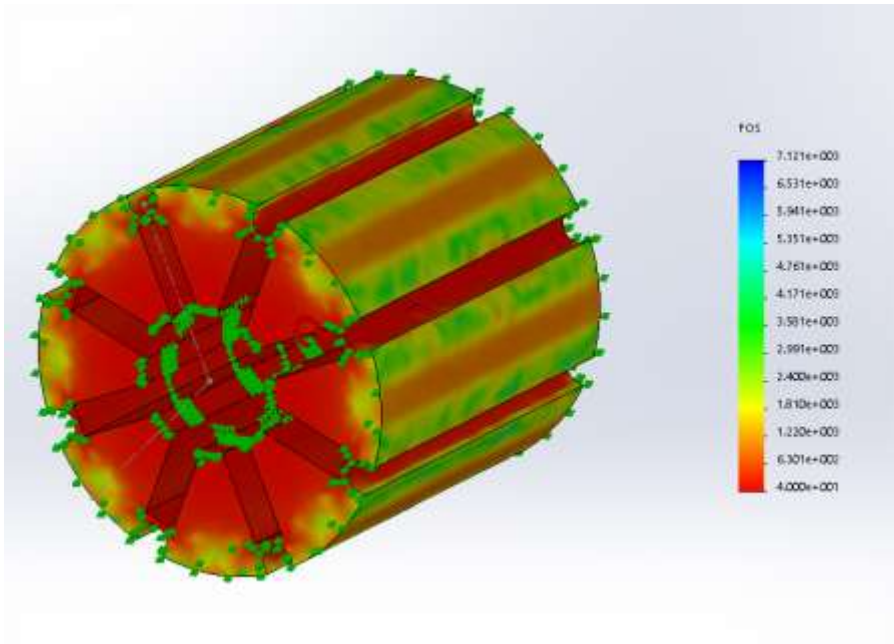


Figure 6.9 - Von Mises stresses on rotor for maximum speed analysis

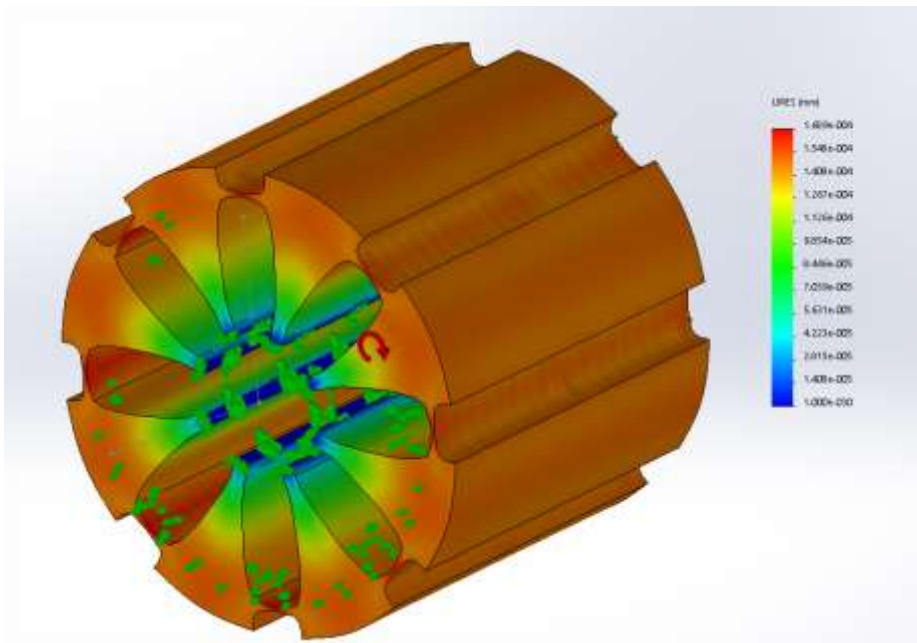


Figure 6.10 - Safety factor on rotor for maximum speed analysis

<u>Load</u>	<u>Max Von Mises (MPa)</u>	<u>Max deformation (mm)</u>	<u>Min Safety Factor</u>
Torsional	11,23	0,00125	18,7
Max speed	5,25	0,00013	40

Table 6.4 - Stress analysis results – rotor

The rotor has way lower stresses and higher safety factors because the way the torque is applied to it, the torque is generated inside the rotor.

Manufacturing

The rotor manufacturing consists one two stages: i) cutting process of the metal sheets; ii) stacking laminations.

- i) There are primarily two ways the lamination cutting: laser beam cutting and stamping machine cutting. The second process is used for achieving high productivity with high-speed stamping machines, but they required specific tools that are not viable to build for just one prototype. This process often left burrs in the lamination's edges.
Laser cutting provides a better cutting quality, low deformation and low residual stress. The drawbacks are its low productive and high cost.
The solution adopted is the laser cutting, it's the better solution for building a prototype and the team also has that kind of service available.
- ii) For stacking the laminations, an auxiliary JIG is required. The design of the shaft was made taking that into account for reducing the overall costs of production by not producing another set of components. The shaft is the stacking JIG.

Fatigue

In materials science, fatigue is the progressive weakening of a material caused by cyclic loadings that creates progressive and localized structural damages and growth of cracks. By each cycle, the crack will continue to grow until it reaches a critical size that occurs when the stress intensity factor of the crack exceeds the fracture toughness of the material. The rotor and shaft are subjected to cyclical loads when used on track. Both will be evaluated together.

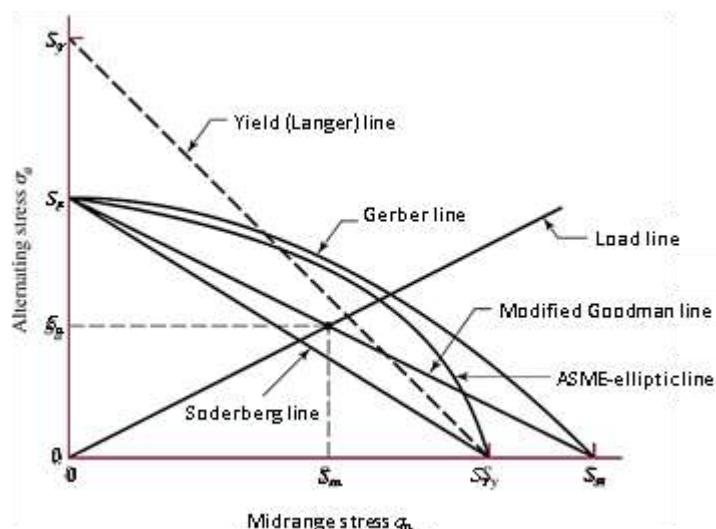


Figure 6.11 - Fatigue Criteria's

Considering a conservative approach – the material data from *Vacodur 49* isn't enough and properties of close cast iron will need be used – the modified Goodman (Figure 6.11) criteria will be used: [22]

$$\frac{\sigma'_a}{S_e} + \frac{\sigma'_m}{S_{ut}} = \frac{1}{n} \quad (6.23)$$

where n is the factor of safety, S_{ut} is the tensile strength of the material and S_e is the endurance limit of the component, σ_m is the mean and σ_a the amplitude stresses. For a hollow shaft we have:

$$\sigma_a = K_f \frac{M_a c}{I} = K_f \frac{32M_a D}{\pi(D^4 - d^4)} \quad (6.24)$$

$$\sigma_m = K_f \frac{M_m c}{I} = K_f \frac{32M_m D}{\pi(D^4 - d^4)} \quad (6.25)$$

$$\tau_a = K_{fs} \frac{T_a c}{J} = K_{fs} \frac{16T_a D}{\pi(D^4 - d^4)} \quad (6.26)$$

$$\tau_m = K_{fs} \frac{T_m c}{J} = K_{fs} \frac{16T_m D}{\pi(D^4 - d^4)} \quad (6.27)$$

$$\sigma_{m \text{ axial}} = K_f \frac{F_z}{A} = K_f \frac{4F_z}{(D^4 - d^4)} \quad (6.28)$$

Also knowing that:

$$\sigma'_a = \sqrt{\sigma_a^2 + 3\tau_a^2} \quad (6.29)$$

$$\sigma'_m = \sqrt{(\sigma_m + \sigma_{axial})^2 + 3\tau_m^2} \quad (6.30)$$

Together with the tensile strength of the material and the loads applied on the components, all that's left to determine is the corrected Endurance limit S_e . It be obtained by:

$$S_e = k_a k_b k_c k_d k_e k_f S_e' \quad (6.31)$$

- $k_a = aS_{ut}^b$ - surface condition modification factor

In which S_{ut} is the minimum tensile strength, a and b established parameters. The surface of both components will be machined, and the material properties considered will belong to the weakest material so: $S_{ut} = 400 \text{ MPa}$, $a = 4,51$ and $b = -0,265 \rightarrow k_a = 0,92$

- k_b = size modification factor

The diameter of the assembly is 60 mm so $k_b = 1,24d^{-0,107} \rightarrow k_b = 0,82$

- k_c = load modification factor

The main stresses will be caused by torsion, so $k_c = 0,59$

- k_d = temperature modification factor

$$k_d = 0.975 + 0.432(10^{-3})T_F - 0.115(10^{-5})T_F^2 + 0.104(10^{-8})T_F^3 - 0.595(10^{-12})T_F^4$$

For a temperature $T_F = 80^\circ\text{C} = 176^\circ\text{F} \rightarrow k_d = 1,02$

- k_e = reliability factor

For a 90% reliability, $k_e = 0.897$

- k_f = miscellaneous-effects modification factor

Not considered.

Using a developed tool using the literature [22] to faster analysis, using the previous equations, the fatigue safety factor is above 1. To trust this result, it would require experimental validation. Assuming the properties of some cast iron due to the lack of information available for the right material and keeping in mind that the rotor is a bunch of laminations stacked together may not be a good approximation.



Figure 6.12 - Exploded view of the final shaft version

The final result of the shaft can be seen at Figure 6.12.

6.3 Stator

The stator is under no relevant mechanical load. In the previous generation, the bridge above the magnets had the need to be dimensioned. The motor theoretically performed better with no bridges, but due to centripetal force while function, a small bridge was mandatory so that the magnet stayed in place. With the new shaft design, having the rods above the magnets, this is no longer a problem. Yet, a small bridge still exists to help the stacking. A small bridge is kept also because stacking eight individual parts of the rotor times 800 laminations and align them perfectly would turn out to be a problem, keeping the bridges solves it. The manufacturing and assembly are performed in the same way as the rotor, but only in this case it's mandatory to build a JIG (Figure 6.13).

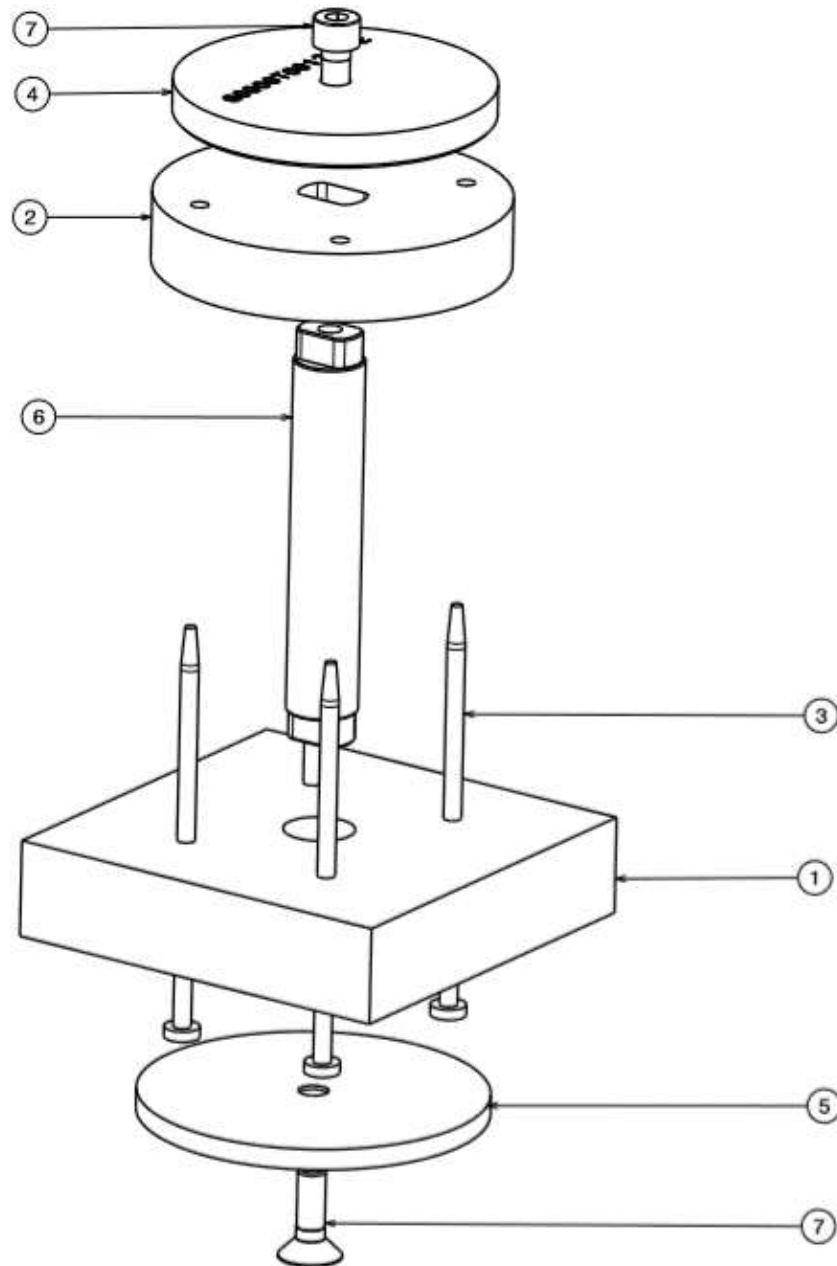


Figure 6.13 - Stator stacking JIG

Winding and Vacuum Pressure Impregnation (VPI)

The winding process like in the tested prototype is to be performed by experts' hands. But performing the VPI is mandatory if the next prototype is to be used in competition. The process guaranties the coils insulation and removes the air between – which helps the heat transfer.

Since the process isn't available in the industry to this size of motors, a solution was prepared: after the coils are inserted in the stator, the last one must be mounted in the housing. After it, the housing will be used as the VPI tank, special lids were designed to turn the housing into a tank. Two extras lids were designed: on to cover the bottom part and one resin entry and one top lead to close the housing and allow to the connection of a pump for air removal.

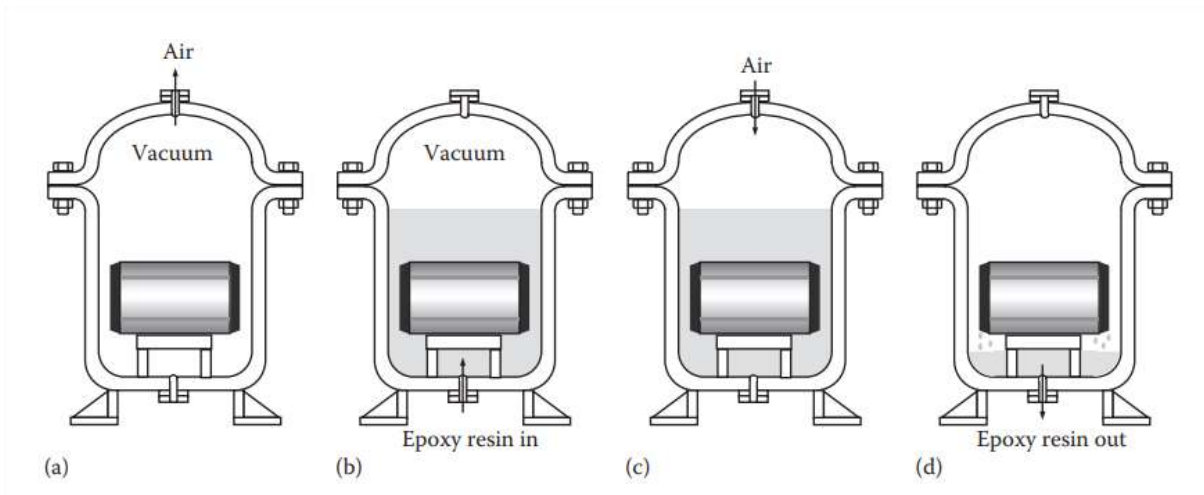


Figure 6.14 - VPI process: (a) evacuating the container into deep vacuum, (b) introducing epoxy resin into the container until the stator is completely submerged, (c) releasing the vacuum of the container and applying pressure over the resin-covered stator to force resin completely into the stator, (d) draining epoxy resin out of the container, and (e) placing the stator into an oven and baking it for curing the epoxy resin (not shown). [7]

6.4 Housing

The materials considered for the shaft are the same for this component. But here, using the titanium alloy isn't that relevant - the housing loads are not that aggressive, no torque applied to any part, it just needs to support its own weight and to withstand the bump load case used with the shaft. This component is also bigger, so getting the same material would rise the costs. While steel is a viable solution, due to its weight it was not considered, leaving aluminum alloys. The team has easy access to AL7570-T6 and, as previous shown before, has excellent properties making it the perfect choice.

The big challenge with the motor housing was to incorporate the cooling housing together, to eliminate the need of plastics and 3D printed components in the motor assembly. The chicane water circuit had better results but it's not possible to accommodate in entirely in the motor housing. A hybrid solution between the chicane and serpent like circuit was the result:



Figure 6.15 Water circuit

Regarding the part protection the stator and rotor, according to Rule T 7.3.2, the housing must have a minimum thickness of 3mm if made of aluminum alloys. The loads on the housing (same as shaft due to bump) are not relevant. But the housing combined with cooling housing can have a few week spots due to its reduced thickness. So, it was important to test how thick it need to be, a force equivalent to letting all motor fall, assuming a 5kg, applied in the weakest spot – the tubing connection - could not cause permanent defects:

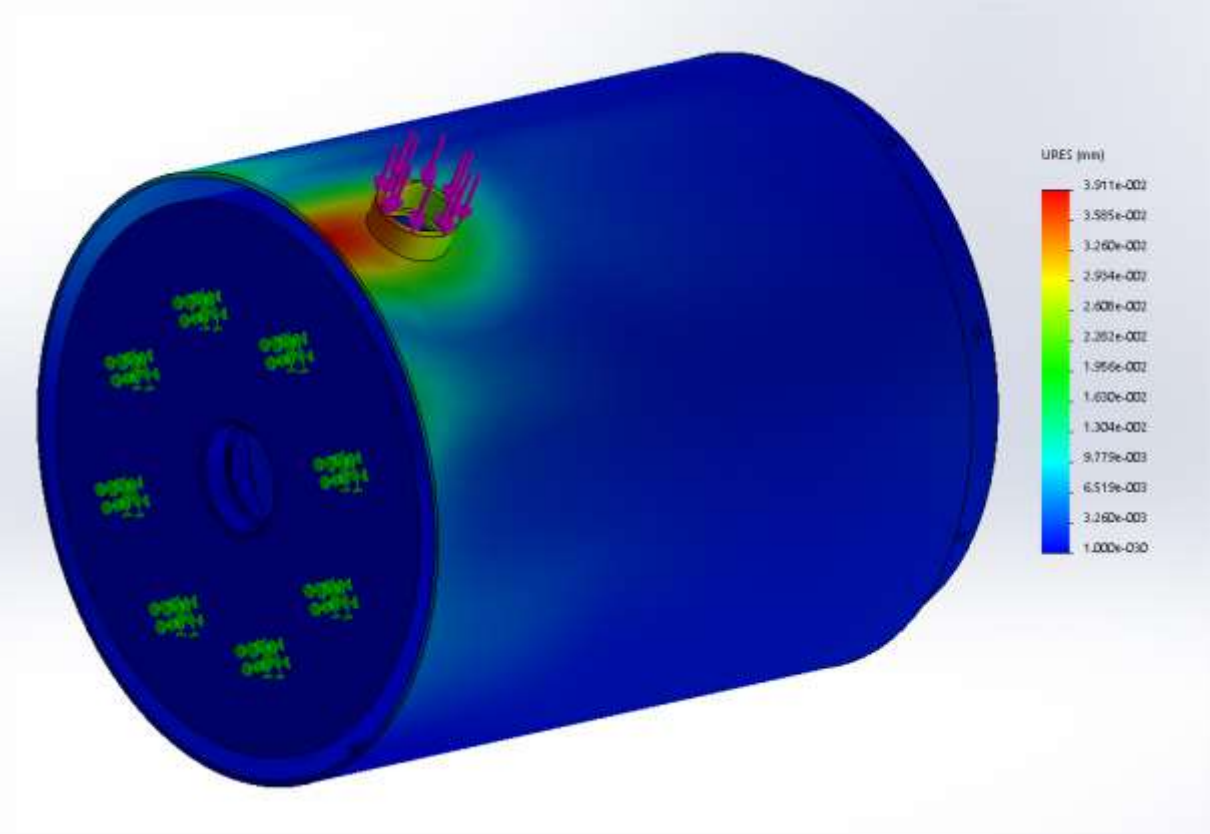


Figure 6.16 - Fall test housing deformation

A small detail regarding the housing, is to have an interior small lug to mount the stator to right place.

This will be the hardest component to machine since it will need two phases: the opening of the circuit channel recurring to EDM and the milling of everything else. Despite not being a requirement, a hard anodization is advised to protect the housing of external conditions, also having the interior anodized, isolates the stator from the housing.

6.5 Lids and supports

The bottom lid makes the bridge to the upright, it has the same number of fasteners for compatibility. Together with the top circuit lid the close the water circuit (Figure 6.17):



Figure 6.17 - Cooling circuit lids

The number of holes for supporting the motor had to be the same as the number that the car upright has. Regarding the motor cover (Figure 6.18), it will be mounted internally to the housing. It must support the top bearing and the motor encoder:

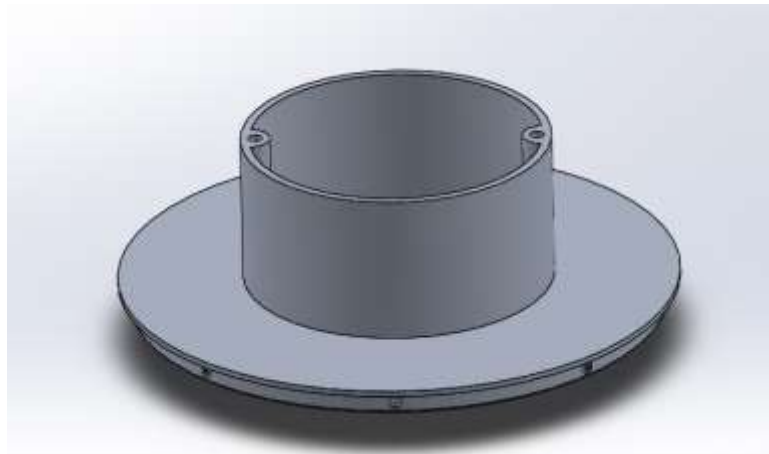


Figure 6.18 - Motor lid

6.6 Bearings and Retainers

The place for the bearings to be mounted at the shaft are part of a section with a 12mm radius. The bearings must withstand a top speed of $20\,000\text{rpm}$, work in temperatures until 75°C and considering an axial force $F_a = 39,2\text{ N}$ and radial force of $F_r = 131,5\text{ N}$.

The bearing for this type of usage needs to be fully closed. It's also important to notice that conventional motor bearings can get "fried" by the electrical current passing through them, causing premature failing by electrical arcing. The solution for this problem is using ceramic ball bearings sealed. This type of bearing offers lower Maintenance costs by expanding its service life. They have an extended grease life since they run colder because of the ceramic balls.

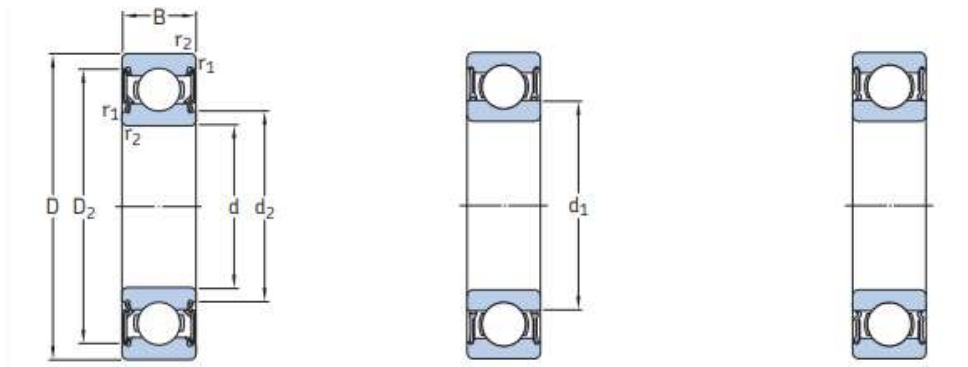


Figure 6.19 - Bearing dimensions

Taking this consideration into account, the select bearing 6201-2RSLTN9/HC5C3WT, which fits the geometrical needs, solves the electrical current problem and can endure the motor speed.

Dimensões principais			Classificações básicas de carga		Limite de carga de fadiga P_u	Classificações de velocidade		Massa	Designação
d	D	B	dinâmica C	estática C_0		Velocidade de referência ¹⁾	Velocidade-limite		
mm			kN		kN	r/min		kg	-
5	16	5	1,14	0,38	0,016	130 000	70 000	0,005	625-2RZTN9/HC5C3WTF1
6	19	6	2,34	0,95	0,04	110 000	60 000	0,008	626-2RSLTN9/HC5C3WTF1
7	19	6	2,34	0,95	0,04	110 000	60 000	0,007	607-2RSLTN9/HC5C3WTF1
	22	7	3,45	1,37	0,057	95 000	53 000	0,012	627-2RSLTN9/HC5C3WTF1
8	22	7	3,45	1,37	0,057	95 000	53 000	0,01	608-2RSLTN9/HC5C3WTF1
10	26	8	4,75	1,96	0,083	85 000	45 000	0,018	6000-2RSLTN9/HC5C3WT
	30	9	5,4	2,36	0,1	75 000	43 000	0,032	6200-2RSLTN9/HC5C3WT
12	28	8	5,4	2,36	0,1	75 000	43 000	0,022	6001-2RSLTN9/HC5C3WT
	32	10	7,28	3,1	0,132	67 000	38 000	0,037	6201-2RSLTN9/HC5C3WT

Figure 6.20 - List of bearings[23]

The dimensions at the previous figure, are used to complete the shaft and lids models.

One face of the motor is in contact with oil transmission, to ensure that no oil enters the motor, a retainer is need:



Figure 6.21 - Retainer dimensions

The choice was the retainer 12X19X5 HMS5 RG1 based of the diameter of the shaft and because it was the retainer available with higher operational speed.

Operating temperature	min.	-40	°C
Operating temperature	max.	100	°C
Permissible operating temperature, short periods	max.	120	°C
Shaft speed	max.	18600	r/min
Shaft surface speed	max.	11.69	m/s

Table 6.5 - Retainer operating conditions

6.7 Engineering fits

Engineering or clearance fits are set during design phase when dimensioning and defining tolerances for a geometric part. It defines the clearance between two mating parts, described as shaft and hole, determining if the parts can move independently from each other, or are temporarily or permanently joined.

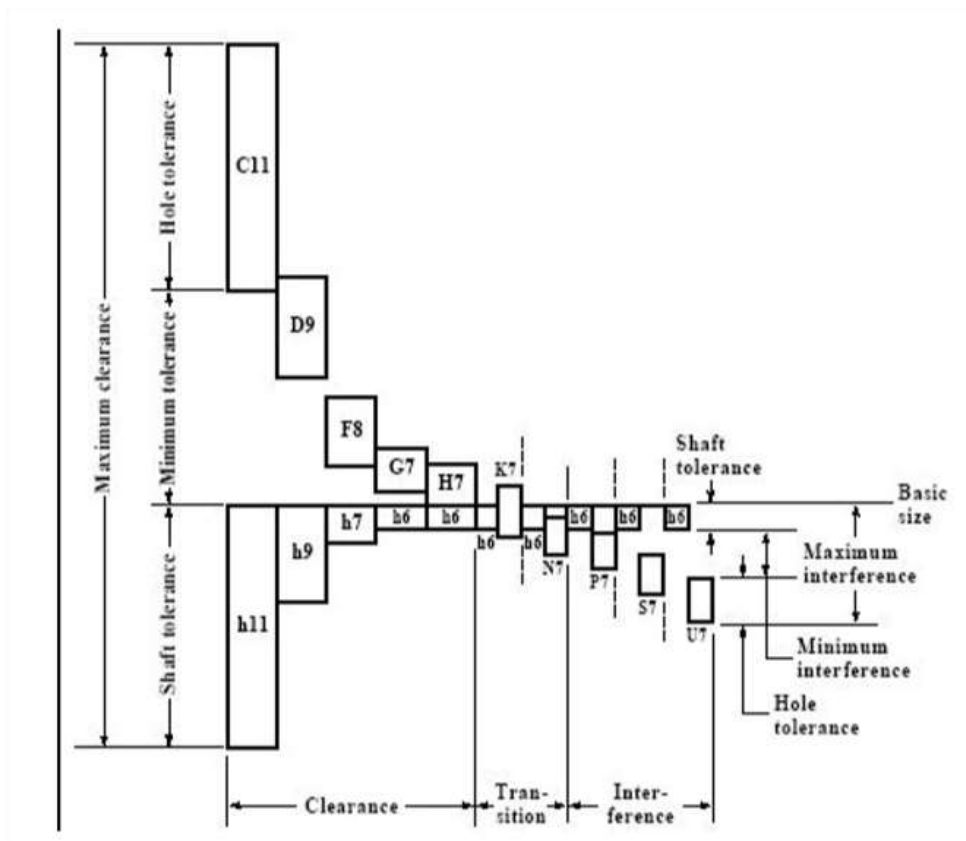


Figure 6.22 - Clearance fit shaft-hole

With all the motor components chose and dimensioned, before preparing its final CAD model and technical drawings, it's necessary to define the clearance between components:

- Stator – housing

This fit must hold the stator in place, but it cannot be too tight, or it will cause losses in the iron magnetic properties. It will be used a press fit with light interference - H7/p6.

- Shaft rods – shaft bottom
The shaft rods need to be held in the right place so they can align properly the laminations for the stacking. A press fit is also the appropriate solution – H7/p6.
- Magnets – rotor
The magnets will be inserted manually, from practical experience, they are too fragile to have any kind of interference fit. A sliding fit is recommended – H7/g6
- Lids – housing
Once the motor is assembled, it's not supposed to disassemble again, but since it's still a prototype a tight interference is need, but one that can be dismounted – fixed fit – H7/n6
- Bearing – shaft
Recommended by seller – j5
- Bearing – housing
Recommended by seller – H7
- Retainer -shaft
Recommended by seller – g6
- Retainer – housing
Recommended by seller – H8

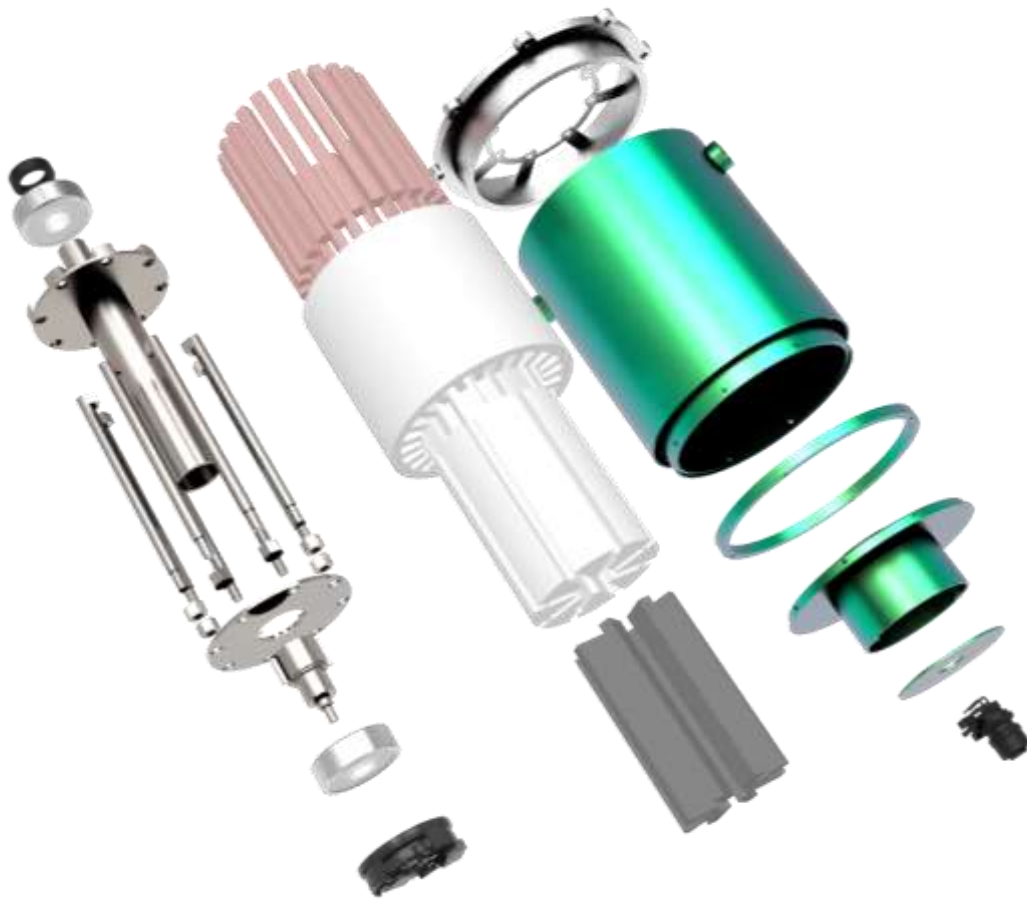


Figure 6.23 - Final CAD model exploded view

6.8 Design, manufacturing, assembling and testing

Every aspect needed to go from scratch to a motor will be listed with estimated durations based on gained experience:

Task	Duration (days)	Begin	Conclusion	Predecessor
<u>Motors</u>	248	01/09/2018 00:00	07/05/2019 00:00	
Electrical	232	01/09/2018 00:00	21/04/2019 00:00	
Initial Parameters	7	01/09/2018 00:00	08/09/2018 00:00	
First Geometry	7	01/09/2018 00:00	08/09/2018 00:00	
Material Selection	7	01/09/2018 00:00	08/09/2018 00:00	
Winding Scheme Configuration	15	01/10/2018 00:00	16/10/2018 00:00	

Electromagnetic 2D simulation	15	01/10/2018 00:00	16/10/2018 00:00	
Thermal Winding Analysis	15	16/10/2018 00:00	31/10/2018 00:00	7
Thermal 3D analysis	15	16/10/2018 00:00	31/10/2018 00:00	7
Winding Bench testing	30	31/10/2018 00:00	30/11/2018 00:00	10
Temperature Sensors (PTCs) arriving	40	10/01/2019 00:00	19/02/2019 00:00	
Workbench Sensors testing	27	13/11/2018 00:00	10/12/2018 00:00	
Winding Company + Thermal paste	21	01/01/2019 00:00	22/01/2019 00:00	
How to apply thermal paste	20	01/01/2019 00:00	21/01/2019 00:00	
Encoders PCB	86	01/01/2019 00:00	28/03/2019 00:00	
Encoders PCB components	41	31/12/2018 00:00	10/02/2019 00:00	
PCB Soldering	7	28/03/2019 00:00	04/04/2019 00:00	17;16
Epoxy Arrival	20	20/01/2019 00:00	09/02/2019 00:00	
Thermal Paste Arrival	20	01/01/2019 00:00	21/01/2019 00:00	
Infrared Sensors	20	01/01/2019 00:00	21/01/2019 00:00	
JIG Design for Thermal Paste	20	01/01/2019 00:00	21/01/2019 00:00	
JIG Printing	11	12/02/2019 00:00	23/02/2019 00:00	22
Acquire Infusion Materials	20	01/01/2019 00:00	21/01/2019 00:00	
JIG Test	1	23/02/2019 00:00	24/02/2019 00:00	23;19;24
Epoxy Demolding	20	01/01/2019 00:00	21/01/2019 00:00	
Winding	21	27/03/2019 00:00	17/04/2019 00:00	11;33;14;19;20;26;15
Epoxy application	4	17/04/2019 00:00	21/04/2019 00:00	27
Encoders arrival	77	29/12/2018 00:00	16/03/2019 00:00	
Magnets arrival	32	05/02/2019 00:00	09/03/2019 00:00	
Mechanical	177	04/11/2018 00:00	30/04/2019 00:00	
Housing Design	40	04/11/2018 00:00	14/12/2018 00:00	
1st Stator Machining	103	14/12/2018 00:00	27/03/2019 00:00	32
1st Rotor Machining	103	14/12/2018 00:00	27/03/2019 00:00	32
1st Shaft Machining	103	14/12/2018 00:00	27/03/2019 00:00	32
1st Housing Machining	103	14/12/2018 00:00	27/03/2019 00:00	32

Epoxy arrival	9	01/04/2019 00:00	10/04/2019 00:00	
Epoxy application	4	10/04/2019 00:00	14/04/2019 00:00	37
Rotor Assembly	11	14/04/2019 00:00	25/04/2019 00:00	33;35;38
Magnets and Plastics Assembly	3	25/04/2019 00:00	28/04/2019 00:00	30;39
Bearings Assembly	2	28/04/2019 00:00	30/04/2019 00:00	40
<u>Motor Assembly</u>	7	30/04/2019 00:00	07/05/2019 00:00	31;3
<u>Test</u>	104	01/01/2019 00:00	15/04/2019 00:00	
Data treatment Interface	80	01/01/2019 00:00	22/03/2019 00:00	
Bench Test Construction	97	08/01/2019 00:00	15/04/2019 00:00	
Electrical Part Design	26	21/01/2019 00:00	16/02/2019 00:00	21
Test bench Assembly	7	15/04/2019 00:00	22/04/2019 00:00	46;45
Without loads	7	07/05/2019 00:00	14/05/2019 00:00	42;47
Loaded Test	14	14/05/2019 00:00	28/05/2019 00:00	48

Table 6.6 - Steps and tasks to design and build a motor

7 Conclusions

7.1 Summary

Building a prototype has an enormous importance. The lessons learned by it helped preventing future problems and they were many in the one built.

Manufacturing of the rotor and stator revealed severe problems for future motor generations: the material didn't have the epoxy to bond the laminations; this led to manually apply the epoxy which cannot be done – the already cut sheet are hard to handle, a lot were damaged and the layer of epoxy was too thick; the epoxy reacts poorly to cold; excess of epoxy covered slots in the stator and in rotor, reducing space for coils and magnets. The only positive aspect regarding this to components were the JIG built for its assembly.

The shaft itself didn't give any problem, its manufacturing by EDM allowed the complex geometry of the rotor. The insertion of the rotor, that was another problem: the excess of epoxy and the damaged laminations due to epoxy hand application, ruined the tolerances for the previous dimensioned fit. This led to a poor process to assemble the rotor, pushing it with a hand press which cause small deformation on one part of the shaft that would later damage a bearing. The most positive aspect was the cooling housing and the motor housing in one component, although smaller parts were used to create the water channels. This showed that could be a viable option.

Assembling the rest of the motor revealed no problem which led finally to testing. A bench test was designed, manufactured and assembled for it. Regarding the tests visual inspection and safety tests were performed before running the motor. After, test using the prototype as generator were performed to determine its characteristics. Soon was found out that the stator and rotor material besides not bringing the epoxy for stacking, it also didn't have the electromagnetic properties right (maybe also mechanics, but those were not tested). The characteristics tested were way lower than what the studies indicated, with all these problems, the model could not be validated.

With all problems found, instead of designing a new generation with specifications custom made for the team's needs, a new one needed to be designed taking every lesson learned and similar to current motors the team uses. This lead to a brainstorm and a lot of concepts, CAD models and even a few plastic prototypes that resulted in four concepts to study of the rotor-stator-shaft geometry and three for the cooling (one of those was the car solution, this one was needed because it was validated and we could compare the other to it).

With electromagnetic and thermal *FEA* models the concept were compared and with the best one, the body of the motor was designed with accordance to the rules. JIGs for parts of its manufacturing were also projected. Critical components of the motor were also studied regarding static loads and fatigue to ensure the next motor doesn't mechanically fail.

Based on this entire experience, to finish a table exported from *Microsoft Project* show every step that is needed to design a motor. It's a process very long with too many variables that one person cannot control.

One final note, every component is oversized if we look only to safety factors, but designed motor will be a validation tool for the team when built and need to endure a lot of bench and car testing. Besides, new problems during the construction will appear, until this process, of designing a motor from scratch until being used in a competition, is fully experience the motor cannot be optimized to save weight, doing this without the mention experience will lead to fails.

7.2 Future work

The next step is to build a new prototype and improve the bench test: testing a new motor is mandatory to validate electromagnetic models and the mechanical design. The prototype tested with the work of this thesis wasn't enough to validate these aspects. Also, there're problems and challenges that only be found out "leaving the paper" and do things.

The bench test needs improvements, while mechanically is prepared to test motors with conditions like the car running, the electrical part need improvement. Do all cabling from scratch, improve safety with emergency stop buttons and design an interface for real-time data treatment.

There are processes better suited for build components like the housing, design possibilities that were not presented in this document made for sintering should be continued to improve.

It would also be interesting in the future to do a topological optimization of the rotor for both mechanics and electromagnetic aspects.



8 References

- [1] J. G. V. V. Sarrico, "Design and Implementation of a 20 kW, 12000 RPM Permanent Magnet Synchronous Motor (PMSM) for the IST Formula Student Powertrain," Master's thesis, Universidade de Lisboa, 2017
- [2] G. A. McCoy, T. Littman, and J. G. Douglass, Energy-Efficient Electric Motor Selection Handbook. Washington: Washington State Energy Office Olympia, 1993, vol. 5.
- [3] A. Fitzgerald, C. Kingsley, and S. Umans, Electric machinery. McGraw-Hill, 2003, vol. 319, no. 4.
- [4] "IPM and SPM machines," [Online]. Available: <https://ei.uni-paderborn.de/en/lea/research/forschungsprojekte/electrical-drives-and-mechatronic-systems/control-of-permanent-magnet-synchronous-motors-for-automotive-applications/>
- [5] A. M. G. & C. AMK, "AMK RACING KIT 4 wheel drive 'Formula Student Electric,'" 2015.
- [6] "FSG Rules 2019," [Online] Available: https://www.formulastudent.de/fileadmin/user_upload/all/2020/rules/FS-Rules_2019_V1.1.pdf
- [7] W. Tong, Mechanical Design of Electric Motors. CRC Press, 2014.
- [8] "Soft Magnetic Cobalt-Iron Alloys," [Online]. Available: https://www.sekels.de/fileadmin/PDF/Englisch/02_soft_magnetic_cobalt_iron_alloys.pdf
- [9] "Neodymium magnets magnetic characteristics," accessed on 13-02-2019. [Online]. Available: <http://www.magmamagnets.com/wp-content/uploads/2017/02/neodymium-magnetic-characteristics.pdf>
- [10] A. Silva, J. Dias, C. T. Ribeiro and L. Sousa, Desenho Técnico Moderno. Lidel, 4ª Edição, 2004
- [11] "The Vacuum Pressure Impregnation Process," [Online] Available: <http://www.sloanelectric.com/vacuum-pressure-impregnation-services/>
- [12] "How To Test Three - Phase AC Motors " [Online] Available: <https://www.electricalengineeringtoolbox.com/2015/12/how-to-test-three-phase-ac-motors.html>
- [13] COMSOL, AC/DC Module User's Guide. COMSOL, 2017.
- [14] "Ansys Fluent Theory Guide" [Online] Available at <https://uiuc-cse.github.io/me498cmfa15/lessons/fluent/refs/ANSYS%20Fluent%20Theory%20Guide.pdf>.
- [15] P. M. de A. Fontes, "Refrigeração do propulsor elétrico de um veículo Formula Student," Master's thesis, Universidade de Lisboa, 2016.
- [16] Materials Properties Handbook: Titanium Alloys, R. Boyer, G. Welsch, and E. W. Collings, eds. ASM International, Materials Park, OH, 1994.
- [17] Metals Handbook, Vol.2 - Properties and Selection: Nonferrous Alloys and Special-Purpose Materials, ASM International 10th Ed. 1990.
- [18] Metals Handbook, Vol. 3, Properties and Selection: Stainless Steels, Tool Materials and Special-Purpose Metals, Ninth Edition, ASM Handbook Committee., American Society for Metals, Materials Park, OH, 1980.
- [19] Structural Alloys Handbook, 1996 edition, John M. (Tim) Holt, Technical Ed; C. Y. Ho, Ed., CINDAS/Purdue University, West Lafayette, IN, 1996.

- [20] "FRICTION, WEAR, AND ADHESION CHARACTERISTICS OF TITANIUM-ALUMINUM ALLOYS IN VACUUM" [Online] Available: <https://ntrs.nasa.gov/archive/nasa/casi.ntrs.nasa.gov/19660006202.pdf>
- [21] "Dimensioning metric screw assemblies" [Online] Available: https://www.wuerth-industrie.com/web/media/en/pictures/wuerthindustrie/technikportal/dinokapitel/Kapitel_06_DINO_techn_Teil.pdf
- [22] J. E. Shigley, C. R. Mischke, and R. G. Budynas, Shigley's Mechanical Engineering Design - 9th. New York: McGraw-Hill, 2011.
- [23] SKF Group, "SKF Rolling Bearings Catalogue." SKF Group, 2013.

9 Appendix

A. Vacodur 49 Datasheet

Preliminary datasheet

VACODUR® 49

STRIP MATERIAL

Composition
49% Co - 2% V - Fe Balance - Nb (present) / ASTM A801 Alloy Type 1

Main properties
Very high saturation induction up to 2.35 T
Adjustable yield strength up to 390 MPa

Applications
High performance motors with maximum power density and low losses

Magnetic properties (typical values)

Coercivity	H_c	50 A/m (optimum magnetic properties) 110 A/m (optimum mechanical properties)
Saturation polarisation	J_s	2.30 T
Maximum permeability	μ_{max}	7.000 (optimum magnetic properties) 15.000 (optimum mechanical properties)
Curie temperature	T_c	950 °C

Static virgin curve (typical values)

Magnetic field strength	H	(kA/m)	0.3	0.8	1.6	4.0	8.0	16
Induction @ $R_{p0.2} = 210$ MPa	B	(T)	1.90	2.10	2.20	2.26	2.28	2.30
Induction @ $R_{p0.2} = 390$ MPa	B	(T)	1.80	2.05	2.15	2.25	2.27	2.30

Iron losses for strip thickness 0.35mm (typical values)

Induction	B	(T)	1.5	1.5	2.0	2.0
Frequency	f	(Hz)	50	400	50	400
Loss @ $R_{p0.2} = 210$ MPa	p_{Fe}	(W/kg)	1.6	31	2.5	60
Loss @ $R_{p0.2} = 390$ MPa	p_{Fe}	(W/kg)	2.9	43	5.0	78

Physical properties (typical values)

Density	ρ	8.12 g/cm ³
Specific electrical resistivity	ρ_s	0.4 $\mu\Omega$ m
Thermal expansion coefficient	α	9.15 · 10 ⁻⁶ 1/K (20...200 °C)

Mechanical properties (typical values)

		optimum magnetic properties	optimum mechanical properties
Tensile strength	R_m	400 MPa	720 MPa
Yield strength	$R_{p0.2}$	210 MPa	390 MPa
Young's Modulus	E	200 GPa	250 GPa
Hardness	HV 10	185	220

Forms of supply and conditions

Strip material	0.05 - 1 mm
Delivery condition	cold rolled with optional coating

Important note: To achieve the typical values a final magnetic annealing is necessary

For optimum magnetic properties: 6h / 880°C, dry hydrogen atmosphere recommended
For optimum mechanical properties: 3h / 750°C, dry hydrogen atmosphere recommended

Preliminary datasheet VACODUR 49

Issue April 2012

Motor-Datenblatt motor data sheet



B. AMK specs datasheet

Bezeichnung/name: **DD5-14-10-POW** - 18600-B5 - Formula Student Datum/date: 15.03.2017
 Teile-Nr./part numbe: **A2370DD** Zeichn.-Nr./drawing no.: 12703-01260

Mechanische Daten mechanical data:
 Gesamtmasse/motor mass "m": 3,55 kg
 Motorträgheitsmoment/inertia "J": 2,74 kgcm²
 Mech. zul. Drehzahl/mech. speed limit "Nmax": 20000 rpm
 Rundlauf/run out (DIN 42955): N
 Wuchtigute/balancing quality: G2,5
 Schwingstärke/vibration level (DIN ISO 2373): N
 Passfeder/shaft key: -

Lagerbelastung bearing load: 
 (Lastangriff Mitte Abtriebswelle)
 (Force to the middle of the shaft): $F_r \uparrow$

A/B - Lager/A/B - side bearing: 6005 / 6003
 GE2 / GE2
 Lagertyp/bearing type: 13000 / 18000 h
 Fettsorte/type of grease: 0 / g
 theo. Fettgedauerdauer/grease life time: 3275 N
 bei Nennrehzahl und 70°C Lageraußenringtemp/rt rated speed and 158°F at outer bearing ring
 erforderliche Fettmenge/necessary grease quantity: 0 / g
 Maximale Axialkraft bei Montage/max. axial force for assembly: 3275 N

A - Lager/A - side bearing: 

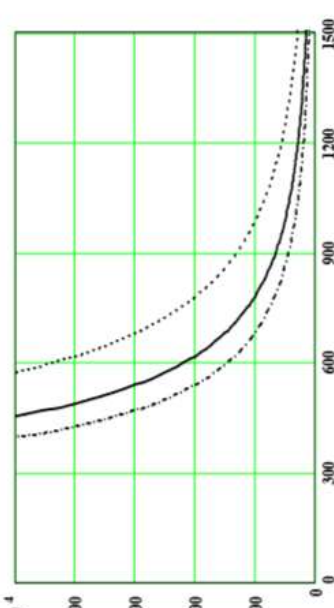
Bremsendaten brake data:
 Typ/type: -
 Bremsmoment/brake torque: Nm
 Bremsstrom/brake current: A
 Bremsenspannung/brake voltage: V
 Spannungsart/voltage type: -
 Einfallzeit/engage time "Te": 0 ms
 max. Bremsenergie/max. braking energy: J
 einmalig/single engagement: J
 Lebenslang/lifetime: -

Lüfterdaten fan data:
 AMK-TNr./AMK part number: -
 Lüfterspannung/fan voltage: V
 Strom/current: A
 Frequenz/frequency: Hz

Lebensdauer / life time [h]

$L_A \left(\frac{F_r}{\text{min}} \right) \frac{6000}{\text{min}}$	8000
$L_A \left(\frac{F_r}{\text{min}} \right) \frac{12000}{\text{min}}$	6000
$L_A \left(\frac{F_r}{\text{min}} \right) \frac{18000}{\text{min}}$	4000

Radialkraft / radial force [N]



Wicklungsschutz thermistor:
 Typ/type: KTY84
 Ansprecht./operation temp: - °C
 Widerstand/resistance (25°C) <= : 629 Ω

Geberdaten position encoder data: **Bemerkungen remarks:**
 AMK-TNr./AMK part number: 108072
 Typ/type: P
 Impulszahl/number of pulses: 262144
 automatisch erstellt, Geber 18 Bit,
 Sonderparameter FSE
 Daten nur gültig mit entsprechender Wasserkühlung

* Typenschildbezeichnung unterstrichen; bitte bei Rückfragen immer angeben /Nameplate data underlined; please state with every inquiry

Ersteller/created by: SMM **Änderungsstand Mechanik/revision motor-mechanics:** 0.00 **Änderungsdatum/motor revision motor date:** 26.10.2016

Für dieses Dokument und die darin enthaltenen Angaben behalten wir uns alle Rechte und technische Änderungen vor.
 All rights reserved for this document and all information included. Technical modifications reserved
 (c) AMK Antriebs- und Steuerungstechnik GmbH Co. KG

C. Motor manufacturing pictures



Figure.9.1 - Stator lamination JIG



Figure.9.2 - Manual application of bonding Epoxy 1



Figure 9.3 - Manual application of bonding Epoxy 2



Figure 9.4 - Dry oven for epoxy cure



Figure 9.5 - Stator after cure



Figure 9.6 - Nitrogen application on shaft



Figure 9.7 - Epoxy application for bonding magnets



Figure 9.8 - Magnets insertion



Figure 9.9 - Damaged stator parts after first attempt of insertion



Figure 9.10 - Final parts before assembling

D. Bench and test pictures

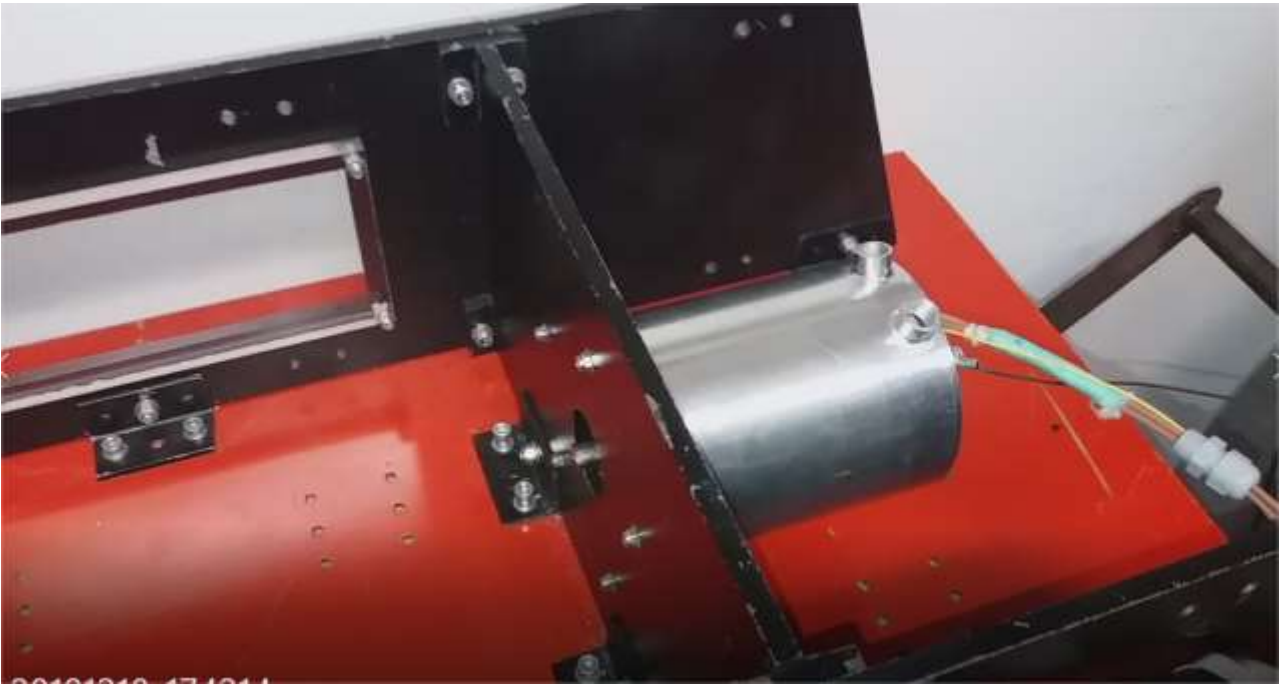


Figure 9.11 - Motor coupled to bench test



Figure 9.12 - Data collection



Figure 9.13 - Data collection 2

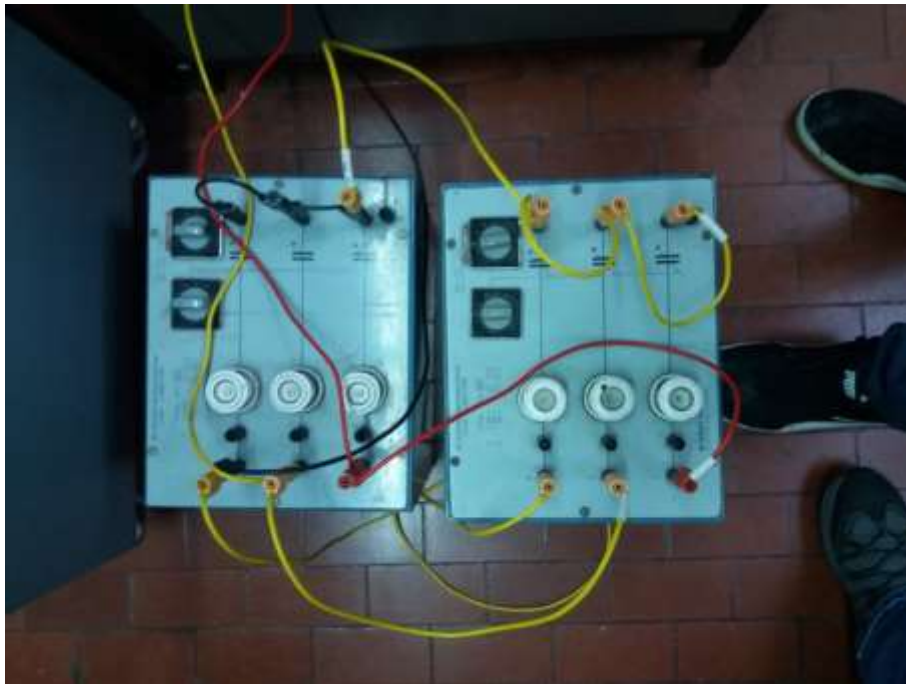
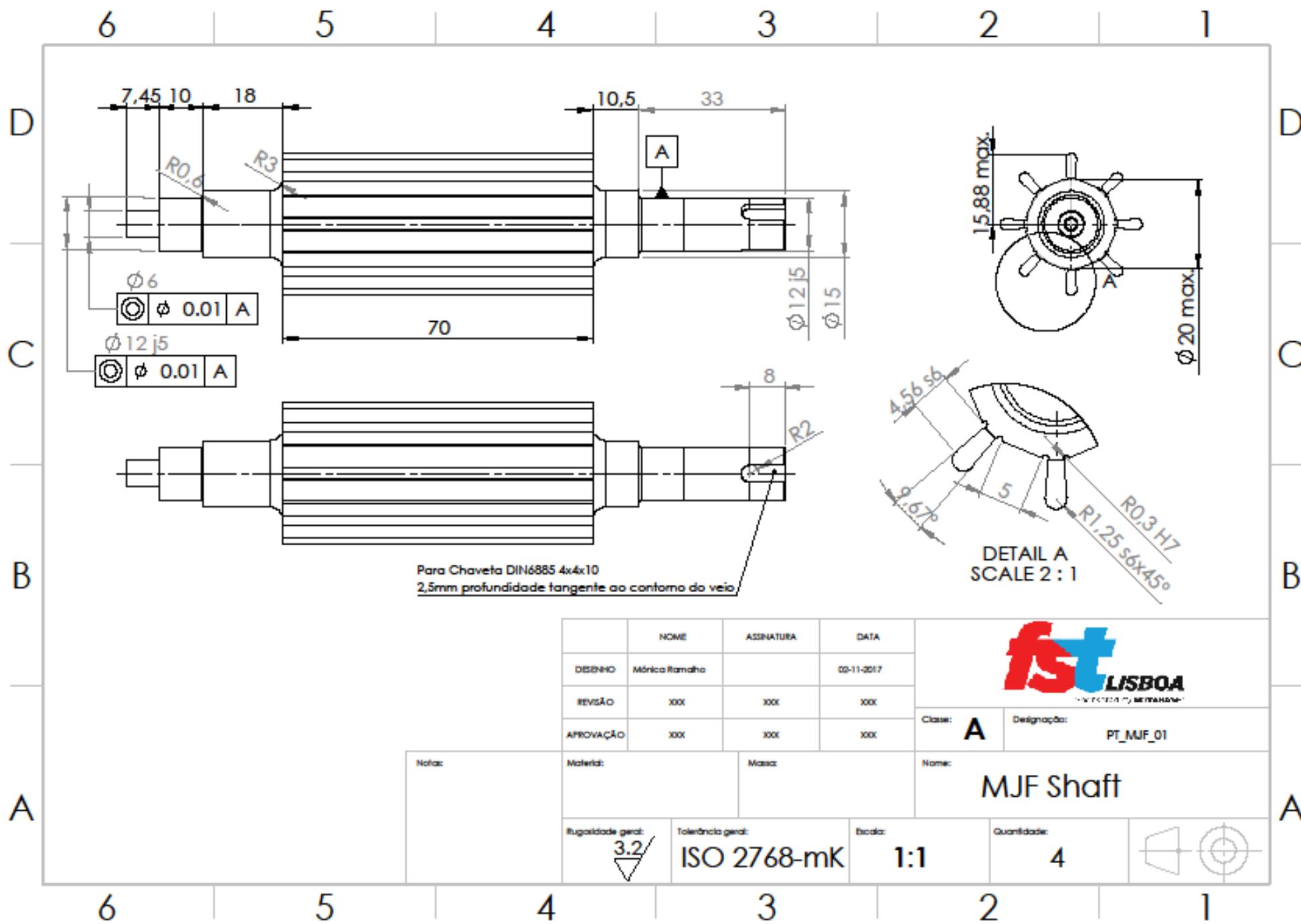


Figure 9.14 - Bench test capacitors

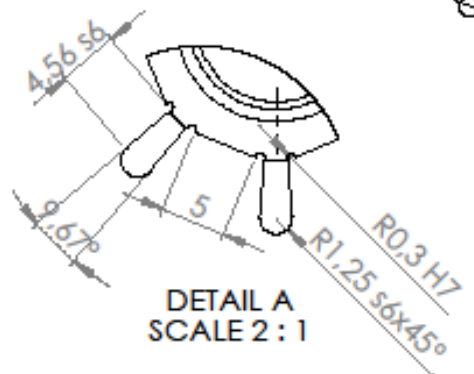


Figure 9.15 - Test bench with Invertors and cooling circuit

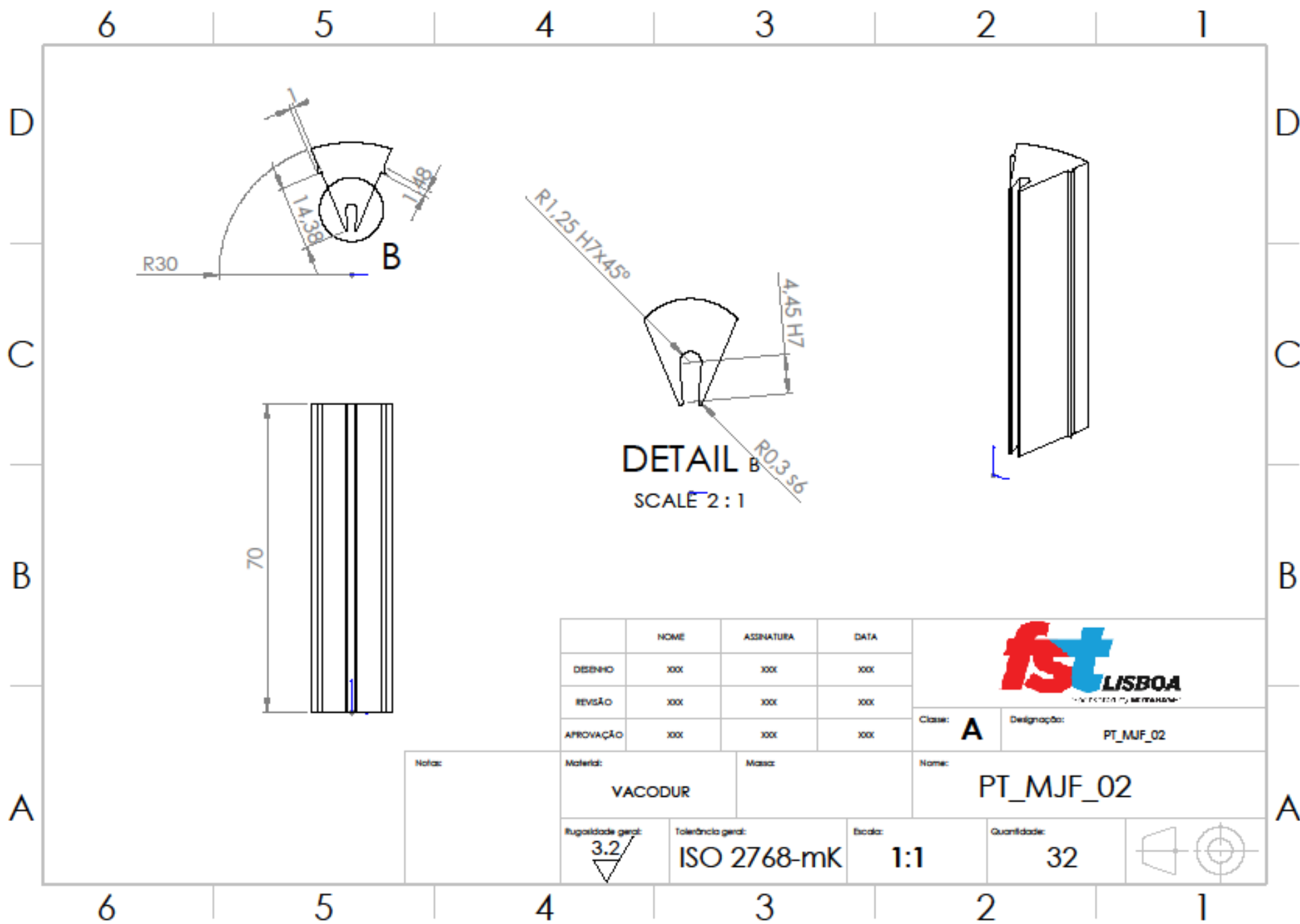
E. Second Generation Technical Drawings



Para Chave DIN6885 4x4x10
 2,5mm profundidade tangente ao contorno do veio



	NOME	ASSINATURA	DATA				
DESENHO	Mónica Ramalho		03-11-2017			Classe: A	Designação: PT_MJF_01
REVISÃO	XXX	XXX	XXX				
APROVAÇÃO	XXX	XXX	XXX				
Notas:	Material:		Massa:		Nome: MJF Shaft		
	Rugosidade gerat: $\sqrt{3.2}$	Tolerância gerat: ISO 2768-mK	Escala: 1:1	Quantidade: 4			



	NOME	ASSINATURA	DATA
DESENHO	xxx	xxx	xxx
REVISÃO	xxx	xxx	xxx
APROVAÇÃO	xxx	xxx	xxx



Classe: **A** Designação: PT_MJF_02

Nome: PT_MJF_02

Material: VACODUR

Massa:

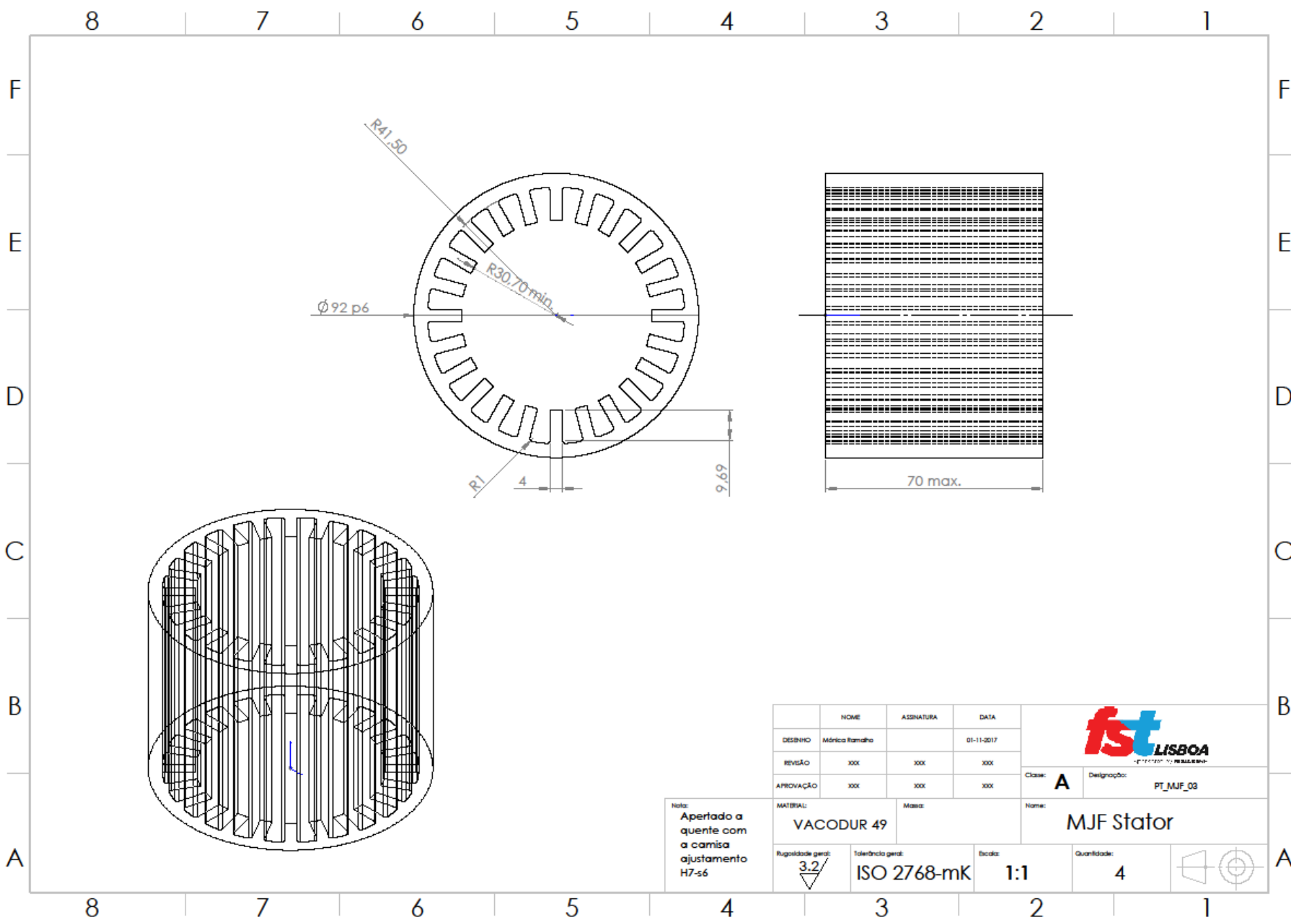
Rugosidade geral: 3.2

Tolerância geral: ISO 2768-mK



Escala: 1:1

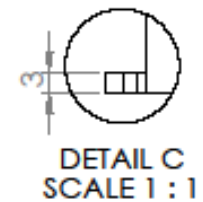
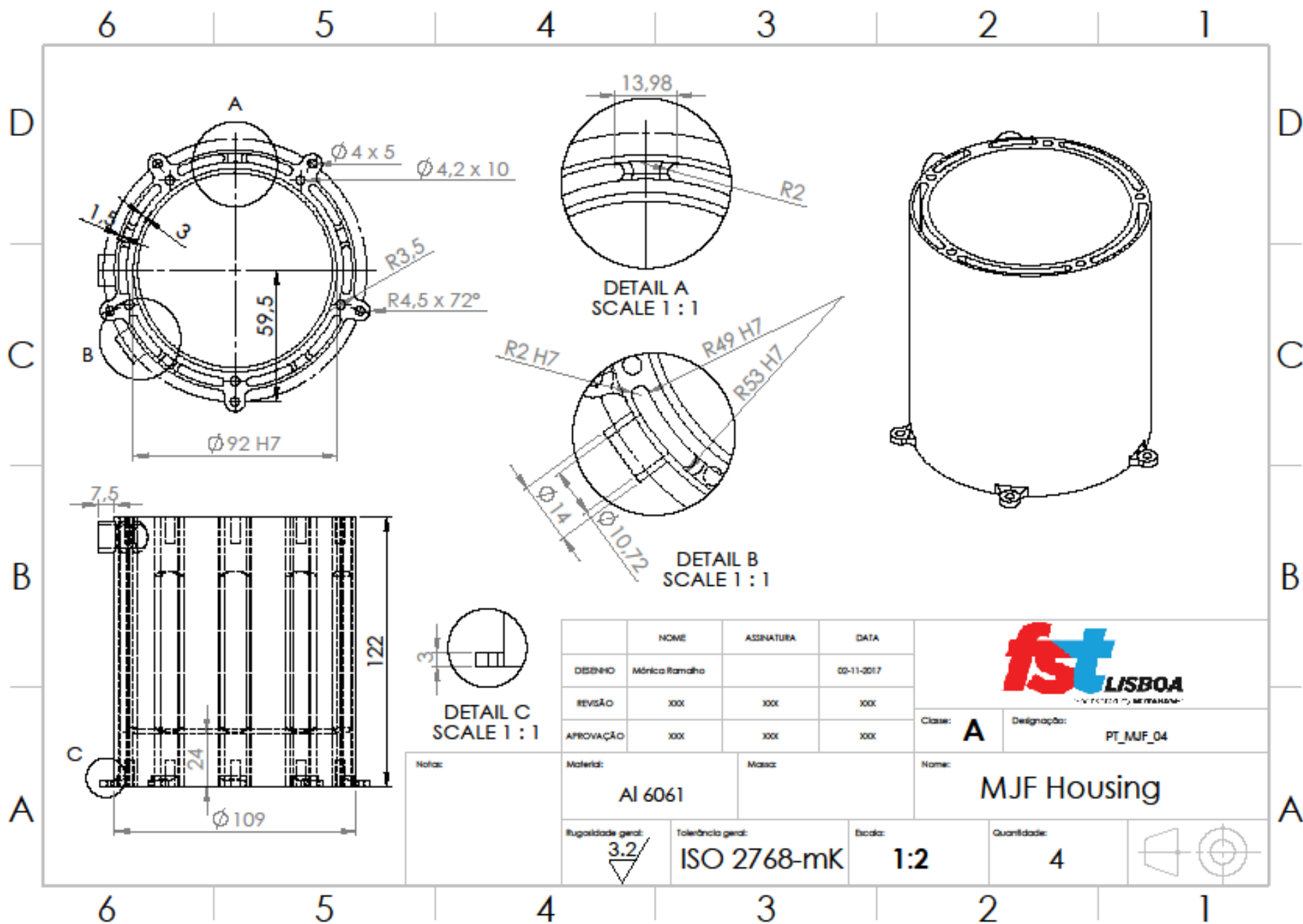
Quantidade: 32





Nota:
Apertado a quente com a camisa ajustamento H7-s6

	NOME	ASSINATURA	DATA				
DESENHO	Mónica Ramalho		01-11-2017			Classe:	A
REVISÃO	xxx	xxx	xxx			Designação:	PT_MJF_03
APROVAÇÃO	xxx	xxx	xxx			Name: MJF Stator	
MATERIAL:		Marca:		Name:			
VACODUR 49				MjF Stator			
Rugosidade gen:	Tolerância gen:	Escala:	Quantidade:				
3.2	ISO 2768-mK	1:1	4				



	NOME	ASSINATURA	DATA
DESENHO	Mónica Ramalho		00-11-2017
REVISÃO	XXX	XXX	XXX
APROVAÇÃO	XXX	XXX	XXX



Class: **A** Designação: PT_MJF_04

Nota:

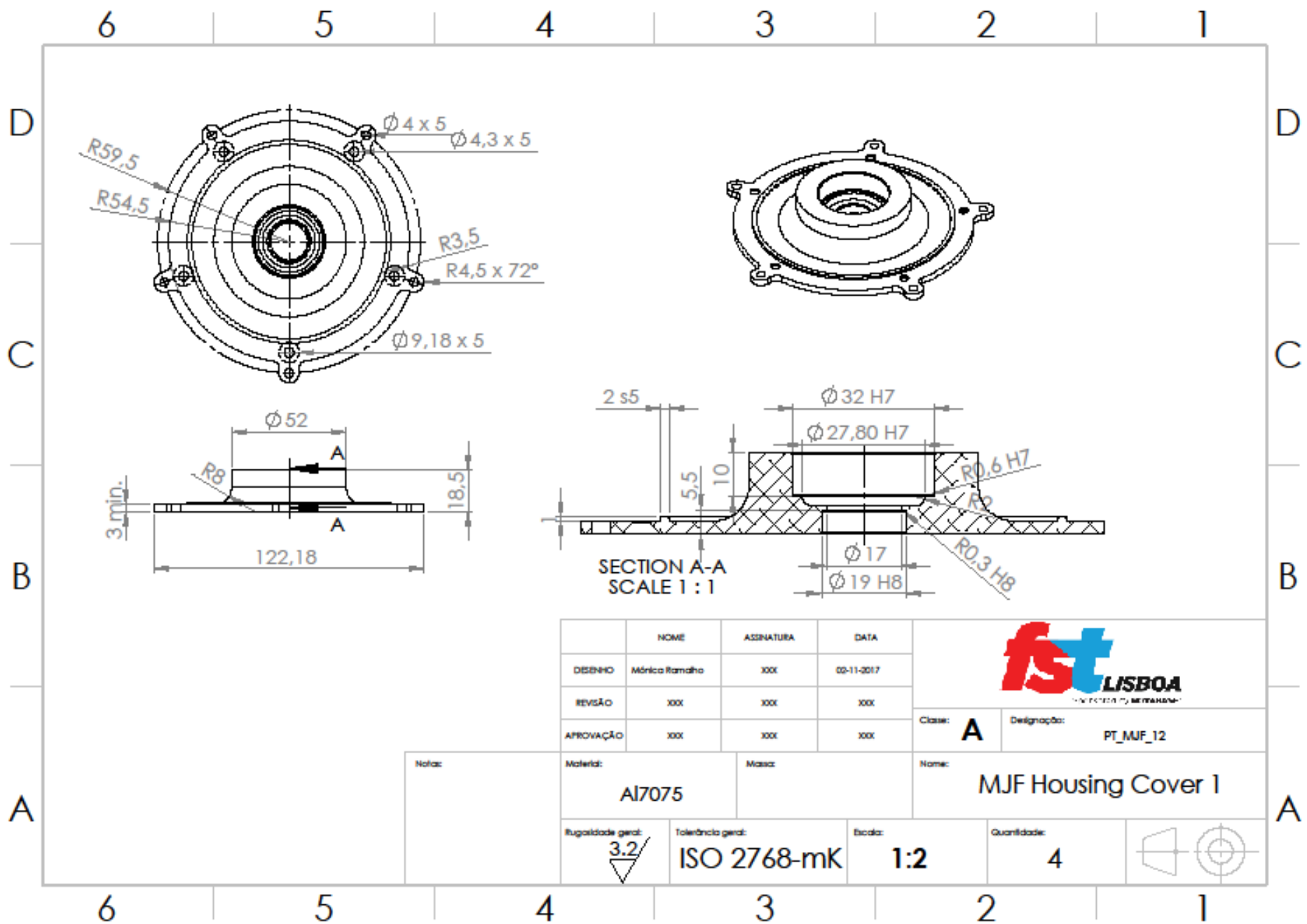
Materia: **Al 6061** Massa:

Nome: **MJF Housing**

Rugosidade geral: **3.2** Tolerância geral: **ISO 2768-mK**

Escala: **1:2** Quantidade: **4**





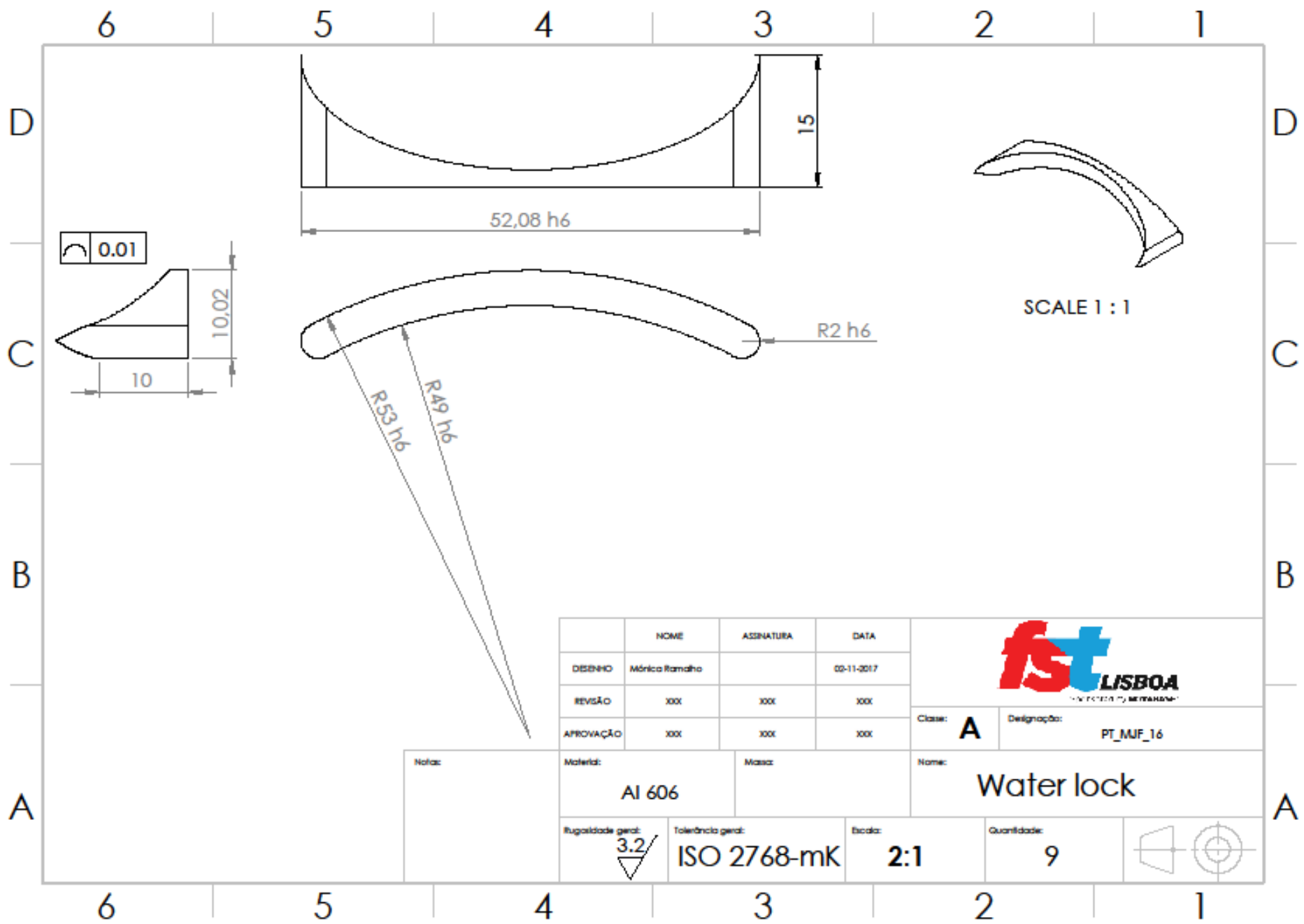
	NOME	ASSINATURA	DATA
DESENHO	Mónica Ramalho	XXX	09-11-2017
REVISÃO	XXX	XXX	XXX
APROVAÇÃO	XXX	XXX	XXX



Classe: **A** Designação: PT_MJF_12

Nome:	Materia:	Massa:	Nome:
	Al7075		MJF Housing Cover 1

Rugosidade geral:	Tolerância geral:	Escala:	Quantidade:	
$3,2$	ISO 2768-mK	1:2	4	



	NOME	ASSINATURA	DATA
DESENHO	Mónica Ramalho		09-11-2017
REVISÃO	XXX	XXX	XXX
APROVAÇÃO	XXX	XXX	XXX

fst LISBOA
INSTITUTO DE INVESTIGACÃO E TRANSFERÊNCIA

Classe: **A** Designação: **PT_MUF_16**

Notas:	Materia: Al 606	Massa:	Nome: Water lock
--------	------------------------	--------	-------------------------

Rugosidade geral: 3.2	Tolerância geral: ISO 2768-mK	Escala: 2:1	Quantidade: 9	
------------------------------	--------------------------------------	--------------------	----------------------	--